cently, Miyanari et al. reported that the association of core protein with the NS proteins and replication complexes around lipid droplets (LDs) is critical for producing infectious viruses (33).

In the present study, we demonstrated that NS5A is a prerequisite for HCV particle production via its interaction with core protein, and we identified serine residues in the C-terminal region of NS5A that play an important role in virion production. Substitution of the serine residues with alanine residues inhibited not only the interaction of NS5A with core protein but also HCV RNA-core association and led to a decrease in HCV particle production with no effect on RNA replication.

MATERIALS AND METHODS

DNA construction. Plasmids pJFH1, which contains the full-length JFH-1 cDNA downstream of the T7 RNA promoter sequence, and pSGR-JFH1/Luc, in which the neomycin resistance gene of pSGR-JFH1 has been replaced by the firefly luciferase reporter gene, have been previously described (24, 56). To generate the fluorochrome gene-tagged full-length JFH-1 plasmid, pJFH1/NS5A-GFP, the region encompassing the RsrII site of NS5A and the BsrGI site of NS5B was amplified by PCR, the amplification product was cloned into pGEM-T Easy vector (Promega, Madison, WI), and the resultant plasmid was designated pGEM-JFH1/RsrII-BsrGI. A GFP reporter gene was amplified by PCR from pGreen Lantern-1 (Invitrogen, Carlsbad, CA) with primers containing the XhoI sequence and inserted, after restriction digestion with XhoI, into the XhoI site of pGEM-JFH1/RsrII-BsrGI. The resulting plasmid was digested by RsrII and BsrGI and ligated into pJFH1 similarly digested by RsrII and BsrGI to produce pJFH1/NS5A-GFP. For generation of the fluorochrome gene-tagged subgenomic reporter plasmid, pJFH1/NS5A-GFP was digested by RsrII and SnaBI and ligated into pSGR-JFH1/Luc similarly digested by RsrII and SnaBI. The mutations in the NS5A gene were generated by oligonucleotide-directed mutagenesis (57). To construct plasmids expressing N-terminally FLAG-tagged HCV core protein or hemagglutinin (HA)-tagged NS5A, DNA fragments encoding core protein or NS5A (wild type or mutants) were generated from the full-length JFH-1 cDNA by PCR. The core protein coding sequence, together with a FLAG sequence linked to its N terminus, was cloned into the pCAGGS vector (37). The coding sequences of NS5A, together with an HA sequence linked to their N termini, were also cloned into pCAGGS vectors. All PCR products were confirmed by automated nucleotide sequencing with an ABI Prism 3130 Avant Genetic Analyzer (Applied Biosystems, Tokyo, Japan).

Cells and viruses. The human hepatoma cell line, Huh-7, and JFH1/4-1 cells, which are Huh-7 cells carrying a subgenomic replicon of JFH-1 (32), were maintained in Dulbecco's modified Eagle's medium (DMEM) supplemented with minimal essential medium nonessential amino acids (Invitrogen), 100 units/ml of penicillin, 100 μg/ml of streptomycin, and 10% fetal bovine serum (FBS) at 37°C in a 5% CO_2 incubator. Huh/c-p7 cells, which are Huh-7 cells stably expressing the proteins core to p7 derived from the JFH-1 strain (18), were incubated in DMEM containing 300 μg/ml of zeocin (Invitrogen). HCV particles derived from JFH-1 were produced by transient transfection of Huh-7 cells with in vitro transcribed RNA, as described previously (56, 58). Recombinant vaccinia virus strain DIs, which expresses the bacteriophage T7 RNA polymerase under the control of the vaccinia virus early/late promoter P7.5, was generated and propagated as previously described (19).

DNA transfection, immunoprecipitation (IP), and immunoblotting. For coexpression of FLAG-tagged core protein and HA-tagged NS5A, cells were seeded onto 35-mm wells of a six-well cell culture plate and cultured overnight. Plasmid DNAs (2 μg) were transfected into cells using TransIT-LT1 transfection reagent (Mirus, Madison, WI). Cells were harvested at 48 h posttransfection, washed three times with 1 ml of ice-cold phosphate-buffered saline (PBS), and suspended in 0.25 ml lysis buffer (20 mM Tris-HCl [pH 7.4] containing 135 mM NaCl, 1% Triton X-100, 0.05% sodium dodecyl sulfate [SDS], and 10% glycerol) supplemented with 50 mM NaF, 5 mM Na_3VO_4, 1 μg/ml leupeptin, and 1 mM phenylmethylsulfonyl fluoride (PMSF). Cell lysates were sonicated at 4°C for 5 min, incubated for 30 min at 4°C, and centrifuged at 14,000 × *g* for 5 min at 4°C. After preclearing, the supernatant was immunoprecipitated with 10 μl of anti-FLAG M2-agarose beads (Sigma, St. Louis, MO). For expression of the full-length HCV polyprotein, Huh-7 cells transfected with 10 μg of in vitro transcribed RNAs by electroporation were resuspended in 20 or 30 ml of culture medium, and 10-ml aliquots were seeded into 100-mm culture dishes. At 72 h posttransfection, the cells were incubated in 0.5 ml of lysis buffer (20 mM Tris-HCl [pH 7.4] containing 135 mM NaCl, 1% Triton X-100, 0.5% sodium deoxycholate, and 10% glycerol) supplemented with 50 mM NaF, 5 mM Na_3VO_4, 1 μg/ml leupeptin, and 1 mM PMSF. After preclearing, the supernatant was immunoprecipitated with 5 μg of polyclonal anti-NS5A antibody (34a) or polyclonal anti-C/EBPβ antibody (Santa Cruz Biotechnology, Santa Cruz, CA), and 20 μl of protein G-agarose beads (Invitrogen). The immunocomplex was precipitated with the beads by centrifugation at 800 × *g* for 30 s and then was washed five times with lysis buffer by centrifugation. The proteins binding to the beads were boiled in 20 μl of SDS sample buffer and then subjected to SDS–12.5% polyacrylamide gel electrophoresis (PAGE). The proteins were transferred onto a polyvinylidene difluoride membrane (Immobilon; Millipore, Bedford, MA) and then reacted with a primary antibody and a secondary horseradish peroxidase-conjugated antibody. The immunocomplexes were visualized with an ECL Plus Western Blotting Detection System (GE Healthcare, Buckinghamshire, United Kingdom) and detected using an LAS-3000 imaging analyzer (Fujifilm, Tokyo, Japan).

In vitro synthesis of HCV RNA and RNA transfection. Plasmid DNAs were digested with XbaI and treated with mung bean nuclease (New England Biolabs, Ipswich, MA) to remove the four terminal nucleotides, resulting in the correct 3′ end of the HCV cDNA. Digested DNAs were purified and used as templates for RNA synthesis. HCV RNA was synthesized in vitro using a MEGAscript T7 kit (Ambion, Austin, TX). Synthesized RNA was treated with DNase I (Ambion), followed by acid guanidinium thiocyanate-phenol-chloroform extraction to remove any remaining template DNA. Synthesized HCV RNAs were used for electroporation. Trypsinized Huh-7 cells were washed with Opti-MEM I reduced-serum medium (Invitrogen) and resuspended at 3×10^6 cells/ml with Cytomix buffer (54). RNA was mixed with 400 μl of cell suspension and transferred into an electroporation cuvette (Precision Universal Cuvettes; Thermo Hybaid, Middlesex, United Kingdom). Cells were then pulsed at 260 V and 950 μF using a Gene Pulser II unit (Bio-Rad, Hercules, CA). Transfected cells were immediately transferred onto six-well culture plates or 100-mm culture dishes.

Luciferase assay. Cells were harvested at different time points posttransfection of subgenomic reporter replicons and lysed in passive lysis buffer (Promega). The luciferase activity in cells was determined using a luciferase assay system (Promega).

Quantification of HCV core protein. HCV core protein in transfected cells or cell culture supernatants was quantified using a highly sensitive enzyme immunoassay (Ortho HCV antigen ELISA Kit; Ortho Clinical Diagnostics, Tokyo, Japan). To determine intracellular core protein amounts, cell lysates were prepared as described previously (41). To determine the efficiency of core protein release, the ratio of extracellular core protein to total core protein (the sum of intra- and extracellular core protein amounts) was calculated.

Intra- and extracellular infectivity assay. Culture supernatants were harvested 72 h posttransfection, and virus titers were determined by a 50% tissue culture infectious dose ($TCID_{50}$) assay as described previously (28, 46). Virus titration was performed by seeding naïve Huh-7 cells in 96-well plates at a density of 1×10^4 cells/well. Samples were serially diluted fivefold in complete growth medium and used to infect the seeded cells (six wells per dilution). At 72 h after infection, the inoculated cells were fixed and immunostained with a mouse monoclonal anti-core protein antibody (2H9) (56), followed by an Alexa Fluor 488-conjugated anti-mouse immunoglobulin G (IgG) (Invitrogen). Wells that showed at least one core protein-expressing cell was counted as positive. Cell-associated infectivity was determined essentially as described previously (12, 47). Briefly, cells were extensively washed with PBS, scraped, and centrifuged for 3 min at 120 × *g*. Cell pellets were resuspended in 1 ml of DMEM containing 10% FBS and subjected to four cycles of freezing and thawing using dry ice and a 37°C water bath. Samples were then centrifuged at 2,400 × *g* for 10 min at 4°C to remove cell debris, and cell-associated infectivity was determined by $TCID_{50}$ assay.

Expression of HCV proteins using vaccinia viruses, metabolic labeling of cells, and radioimmunoprecipitation analysis. Metabolic labeling of cells and radioimmunoprecipitation analysis were performed as described by Huang et al. (17) with some modifications. A total of 4×10^5 Huh-7 cells were seeded onto each well of six-well cell culture plates and cultured overnight. A 2-μg amount of subgenomic replicon DNAs carrying defined NS5A mutations was transfected into cells using TransIT-LT1 transfection reagent, and at 12 h posttransfection the cells were then infected at a multiplicity of infection of 10 with recombinant vaccinia viruses expressing the T7 RNA polymerase. After 40 h of transfection, cells were incubated in methionine- and cysteine-deficient DMEM (Invitrogen) or phosphate-deficient DMEM (Invitrogen) for 2 h and labeled for 6 h with [^{35}S]methionine and [^{35}S]cysteine (200 μCi/well; GE Healthcare) or

[^{32}P]orthophosphate (250 μCi/well; GE Healthcare). The cells were then washed twice with cold PBS and lysed with SDS lysis buffer (50 mM Tris-HCl [pH 7.6], 0.5% SDS, 1 mM EDTA, 20 μg/ml of PMSF). The cell lysates were passed through a 27-gauge needle several times to shear cellular DNA. After a 10-min incubation at 75°C, the lysates were clarified by centrifugation and diluted five-fold with HNAET buffer (50 mM HEPES [pH 7.5], 150 mM NaCl, 0.67% bovine serum albumin, 1 mM EDTA, 0.33% Triton X-100). After preclearing by incubation with 20 μl of protein G-agarose beads for 1 h at 4°C, the supernatant was incubated with 2 μg of rabbit polyclonal anti-NS5A antibody overnight at 4°C. A 20-μl aliquot of protein G agarose beads was further added and incubated for 2 h at 4°C. The cell pellets were washed three times with 0.5 ml of HNAETS buffer (HNAET containing 0.5% SDS), followed by washing once with 0.5 ml of HNE buffer (50 mM HEPES [pH 7.5], 150 mM NaCl and 1 mM EDTA). After treatment with or without λ protein phosphatase (New England Biolabs), the cell pellets were suspended in 20 μl of SDS sample buffer and boiled for 10 min. The proteins were resolved on 10% SDS-polyacrylamide gels and analyzed by autoradiography.

Subcellular fractionation analysis. All steps were carried out at 4°C in the presence of a protease inhibitor cocktail (Complete; Roche, Mannheim, Germany) as described previously (20), with some modifications. Cells were suspended in four cell volumes of homogenization buffer (50 mM NaCl, 10 mM triethylamine [pH 7.4], 1 mM EDTA), snap frozen in liquid nitrogen, stored at −80°C, and thawed in a water bath at room temperature. Supernatants (0.4 ml) were layered on linear 10-ml iodixanol gradients from 2.5 to 25% and centrifuged at 37,000 rpm for 3.5 h in an SW41 rotor (Beckman, Fullerton, CA), followed by collection of 0.8-ml fractions from the top. Each fraction was concentrated by Centricon YM30 (Millipore), separated by SDS-PAGE, and immunoblotted with a rabbit polyclonal anti-calnexin antibody (Stressgen Biotechnologies, Victoria, Canada), a mouse monoclonal anti-adipose differentiation-related protein (ADRP) antibody (Progen Biotechnik, Heidelberg, Germany), or a rabbit polyclonal anti-NS5A antibody. The core protein amount in each fraction was also determined by enzyme-linked immunosorbent assay (ELISA).

IP-RT-PCR. The process of cell lysis to RNA purification was carried out essentially as described by Johnson et al. (21) with some modifications. A total of 3×10^6 Huh-7 cells were transfected with 10 μg of in vitro transcribed HCV RNAs and resuspended in 20 or 30 ml of culture medium, after which 10-ml aliquots were seeded into 100-mm culture dishes. At 72 h posttransfection, the cells were scraped and incubated in 500 μl of hypotonic buffer (10 mM HEPES [pH 7.6], 1.5 mM $MgCl_2$, 10 mM KCl, 0.2 mM PMSF) per dish. The cells were passed through a 20-gauge needle several times, lysed with Nonidet P-40 at a final concentration of 1%, and incubated on ice for an additional 10 min. After centrifugation at 4,000 × *g* at 4°C for 15 min, glycerol was added to the supernatants at a final concentration of 5%. The cell lysates were incubated with 20 μl of protein G-agarose beads for 30 min at room temperature. After the cell lysates were removed from protein G-agarose beads, 5 μg of mouse monoclonal anti-core protein antibody or normal mouse IgG (Sigma) as a negative control was added, and samples were incubated for an additional 1 h at room temperature. A 20-μl aliquot of protein G-agarose beads per sample was added to the cell lysates and incubated for 1 h. After incubation, the beads were washed three times with wash buffer (10 mM Tris-HCl [pH 7.6], 100 mM KCl, 5 mM $MgCl_2$, and 1 mM dithiothreitol) and eluted in 100 μl of elution buffer (50 mM Tris-HCl [pH 8.0], 1% SDS, and 10 mM EDTA) at 65°C for 10 min. After treatment with 100 μg of proteinase K at 37°C for 30 min, the RNAs in immunocomplexes were isolated by acid guanidinium thiocyanate-phenol-chloroform extraction. Reverse transcriptase PCR (RT-PCR) was carried out using random hexamer and Superscript II RT (Invitrogen), followed by nested PCR with LA *Taq* DNA polymerase (TaKaRa, Shiga, Japan) and primer sets amplifying the fragments of nucleotides (nt) 129 to 2367 and nt 7267 to 9463 of the JFH-1 genome. To amplify the fragment of nt 129 to 2367, the sense primer 5′-CTGTGAGGAACTACTGTCTT-3′ and the antisense primer 5′-TCCACGATGTTCTGGTGAAG-3′ were used for first-round PCR; the sense primer 5′-CGGGAGAGCCATAGTGG-3′ and the antisense primer 5′-CATTCCGTGGTAGAGTGCA-3′ were used for second-round PCR. To amplify the fragment of nt 7267 to 9463, the sense primer 5′-GTCCAGGGTGCCCGTTCTGGACT-3′ and the antisense primer 5′-GCGGCTCACGGACCTTTCAC-3′ were used for first-round PCR; the sense primer 5′-CACCGTTGCTGGTTGTGCT-3′ and the antisense primer 5′-GTGTACCTAGTGTGTGCCGCTCTA-3′ were used for second-round PCR.

Indirect immunofluorescence analysis. Cells incubated for 3 days after transfection with JFH-1 RNAs were seeded in an eight-well chamber slide (BD Biosciences, San Jose, CA) and cultured overnight. The adherent cells were washed twice with PBS and fixed with 4% paraformaldehyde at room temperature. After a washing step with PBS, the cells were permeabilized with PBS containing 0.3% Triton X-100 and 2% FBS for 1 h at room temperature and stained with a rabbit polyclonal anti-NS5A antibody and a mouse monoclonal anti-core protein antibody. The fluorescent secondary antibodies were Alexa Fluor 488- or Alexa Fluor 555-conjugated anti-rabbit or anti-mouse IgG antibodies (Invitrogen). Analyses of JFH-1 were performed on a Zeiss confocal laser scanning microscope LSM 510 (Carl Zeiss, Oberkochen, Germany).

RESULTS

Mutations of serine residues at the NS5A C terminus impair basal phosphorylation but have little effect on viral RNA replication. As demonstrated in a previous study, insertion of GFP into the NS5A C terminus does not significantly affect viral RNA replication but reduces the generation of infectious HCV particles (41). The C-terminal region of NS5A contains highly conserved serine residues that are involved in basal phosphorylation (1, 23, 49). To examine the involvement of the serine clusters (cluster 3-A [CL3A] and cluster 3-B [CL3B]) in the C-terminal region of NS5A in HCV particle production, we created mutated HCV genomes as well as subgenomic replicons carrying alanine substitutions for the conserved serine residues at aa 2384, 2388, 2390, and 2391 (residues are numbered according to the positions within the original JFH-1 polyprotein) (CL3A/SA); at aa 2428, 2430, and 2433 (CL3B/SA); or an in-frame deletion spanning aa 2384 to 2433 (Δ2384–2433) (Fig. 1). A construct with an in-frame insertion of GFP (NS5A-GFP) was also generated as described previously for the Con1 isolate (34).

First, we analyzed the effects of the NS5A mutations on HCV RNA replication using a transient RNA replication assay using subgenomic luciferase reporter replicons (Fig. 2A) and found that the serine-to-alanine substitutions (CL3A/SA and CL3B/SA) did not affect viral RNA replication. NS5A-GFP and Δ2384–2433 slightly reduced RNA replication, indicating that the mutations of the NS5A C terminus tested in this study do not critically affect RNA replication, which is consistent with previous reports (1, 34, 51).

Next, the phosphorylation status of the mutated NS5A was analyzed as described in Materials and Methods (Fig. 2B). NS5A was isolated from radiolabeled cells by IP and analyzed either directly by SDS-PAGE or after treatment with λ protein phosphatase. Analysis of ^{32}P-radiolabeled proteins revealed that the CL3A/SA, CL3B/SA, and Δ2384–2433 mutations resulted in marked reduction of basal phosphorylation (Fig. 2B, compare lane 1 with lanes 3, 5, and 7 in the top panel). All ^{32}P-labeled NS5A proteins were sensitive to treatment with phosphatase (lanes 2, 4, 6, and 8). The possibility that loss of signal after dephosphorylation was due to contaminating proteases present in the phosphatase preparations can be ruled out because no degradation of the ^{35}S-labeled proteins was observed (Fig. 2B, bottom panel). These results suggest that mutations in the C-terminal serine cluster of NS5A impair basal phosphorylation but have no significant effect on viral RNA replication.

Effect of mutations introduced into the NS5A C terminus on the production of infectious HCV particles. To analyze HCV particle production from cells transfected with the in vitro transcribed viral genomic RNAs, we harvested supernatants and cells at 4, 24, 48, 72, and 96 h posttransfection and measured the amounts of core protein. As shown in Fig. 3A, comparable amounts of core proteins were detected in all transfected cells 4 h after transfection, reflecting unchanged

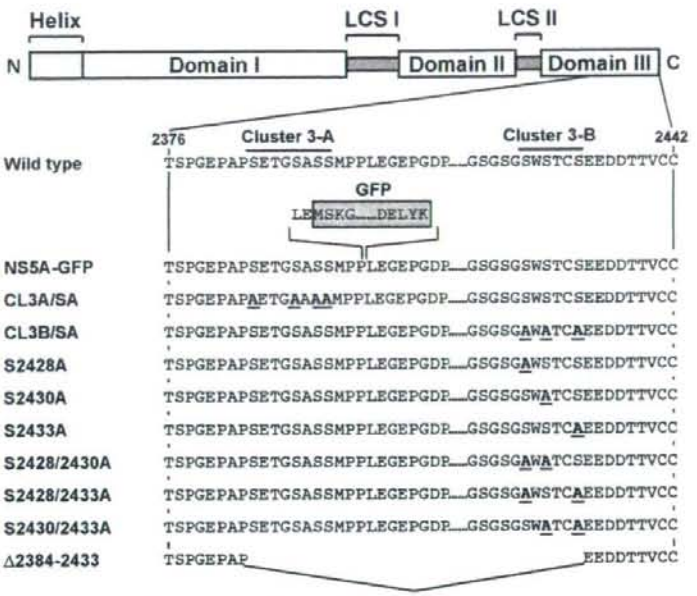

FIG. 1. Structures of HCV constructs used in this study. Schematic diagram of the NS5A structure according to Tellinghuisen et al. (52) is shown in the top panel. The three domains are indicated by white boxes and are separated by trypsin-sensitive regions with presumably low structural complexity (low-complexity sequence [LCS]). The numbers indicate amino acid residues within the original JFH-1 polyprotein. The names listed on the left represent full-length HCV constructs, subgenomic reporter replicons, or N-terminally HA-tagged NS5A constructs used in this study. NS5A-GFP carries a GFP insertion between aa 2394 and 2395 as indicated by a shaded box. CL3A/SA and CL3B/SA carry several serine-to-alanine substitutions in the NS5A C terminus constructed as described previously (1). HCV constructs from S2428A to S2430/2433A carry single or double serine-to-alanine substitutions generated by modification of the CL3B/SA construct. The Δ2384–2433 mutant possesses an in-frame deletion in the C-terminal region of NS5A. Amino acid substitutions are marked in bold and underlined. N and C represent N terminus and C terminus, respectively.

transfection efficiencies, and the kinetics of intracellular core protein levels was similar among transfectants. By contrast, core protein released from cells transfected either with the mutated genome of CL3B/SA, Δ2384–2433, or NS5A-GFP was more than 10-fold lower than that for the wild-type JFH-1 or CL3A/SA (Fig. 3B). Figure 3C shows the efficiency of core protein release from each transfectant, which is expressed as a percentage of the extracellular core protein level relative to the amount of total core protein (the sum of intra- and extracellular core protein). Core protein release efficiency with the wild type and CL3A/SA was 2 to 13% at 48 to 96 h after transfection, while only 1% or less of core protein was released in the cases of CL3B/SA, Δ2384–2433, and NS5A-GFP strains.

To further investigate production and release of infectious virus particles, naïve Huh-7 cells were infected with culture supernatants of cells harvested 72 h posttransfection, and infectious virus titers were determined by $TCID_{50}$ assay at 72 h after infection. Figure 3D shows that release of infectious virus particles from cells transfected with the genome of CL3B/SA or Δ2384–2433 mutants was markedly reduced (about 10,000-fold) compared to that from wild-type- or CL3A/SA-transfected cells (white bars). To examine whether such a decrease in infectious HCV in the culture supernatants was attributable to defective virion assembly or impaired release of virions, we determined cell-associated infectivity (Fig. 3D). Production of intracellular infectious virions in CL3B/SA- and Δ2384-2433-transfected cells was strongly impaired in comparison with that in wild-type-transfected (~1,000-fold) and CL3A/SA-transfected (~100-fold) cells. Thus, the results suggest a potential role for the serine cluster at aa 2428, 2430, and 2433 of NS5A in assembly of infectious HCV particles. Among the NS5A mutations tested, CL3B/SA is of particular interest because this mutation leads to a marked reduction in HCV production with no impact on viral RNA replication.

Serine residues at aa 2428, 2430, and 2433 are important for the interaction between NS5A and core protein. Miyanari et al. reported that the association of core protein with NS proteins is critical for infectious HCV production and that mutations of the core protein and NS5A that cause these proteins to fail to associate with each other impair the production of infectious virus (33). Based on these observations and the findings noted above, we hypothesize that NS5A plays a key role in recruiting viral RNA, which is synthesized at the viral replication complex, to nucleocapsid formation via interaction between the NS5A C-terminal region and the core protein. To prove this, we analyzed the interaction of NS5A with the core protein by coimmunoprecipitation experiments. HA-tagged NS5A constructs carrying defined mutations were generated (Fig. 1) and coexpressed with the FLAG-tagged core protein in Huh-7 cells. As shown in Fig. 4A, coimmunoprecipitation of NS5A

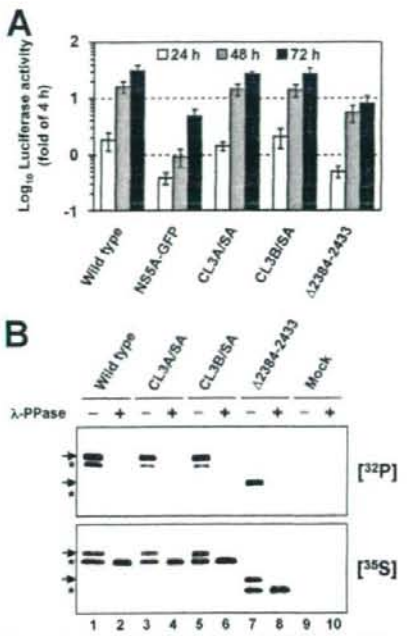

FIG. 2. Mutations at the C terminus of NS5A impair basal phosphorylation and have only a minor impact on RNA replication. (A) Replication of given mutants in transfected Huh-7 cells as determined by luciferase reporter assays performed at 24, 48, and 72 h posttransfection (white, gray, and black bars, respectively). Values given were normalized for transfection efficiency using the luciferase activity determined 4 h after transfection, which was set to 1. Mean values of quadruplicate measurements and the standard deviations are given. (B) Phosphorylation analysis of NS5A using the vaccinia virus T7 hybrid system. NS3-to-NS5B polyprotein fragments carrying the mutations specified above the lanes were transfected into Huh-7 cells, and proteins were radiolabeled with [^{32}P]orthophosphate or [^{35}S]methionine and [^{35}S]cysteine. NS5A proteins were isolated by IP and separated by SDS-PAGE (10% polyacrylamide). Mock-transfected cells served as a negative control (lanes 9 and 10). Half of the samples were treated with λ protein phosphatase (λ-PPase) (+) whereas the other half was mock treated (−) prior to SDS-PAGE. Arrows and asterisks indicate hyperphosphorylated and basally phosphorylated forms, respectively.

with the core protein was observed in cells expressing the wild-type NS5A and the CL3A/SA-mutated NS5A, but the amount of immunoprecipitated NS5A in the CL3A/SA-expressing cells was slightly lower than that in the wild-type-expressing cells. In contrast, the CL3B/SA- or the Δ2384-2433-mutated NS5A coimmunoprecipitated with the core protein only slightly or not at all.

We further examined the interaction of NS5A with core protein in cells expressing HCV genomes. At 72 h posttransfection with the wild type or CL3B/SA, cells were harvested and immunoprecipitated with an anti-NS5A antibody or an anti-C/EBPβ antibody as a negative control, followed by immunoblotting. Under these experimental conditions, the amount of extracellular core protein released from cells transfected with the CL3B/SA genome was about 10-fold lower than that for the wild type, although comparable amounts of intracellular core protein were observed in both transfectants (Fig. 4B, left panels). As shown in the right panels of Fig. 4B, the core protein was specifically coimmunoprecipitated with NS5A in cells expressing the wild-type JFH-1 genome but not with the mutated NS5A in cells expressing the CL3B/SA genome. These results demonstrate that NS5A interacts with the core protein in cells producing infectious particles and that serine residues at aa 2428, 2430, and 2433 are important to the success of this interaction.

Two serine residues among aa 2428, 2430, and 2433 are responsible for regulating the interaction of NS5A with the core protein as well as HCV particle production. To further determine the critical residues in the C-terminal serine cluster of NS5A responsible for HCV particle production, we replaced one or two serine residues in the region with alanine (Fig. 1) and investigated which serine-to-alanine substitution influenced HCV particle production. Core protein levels in cells transfected with any construct were comparable over 4 days after transfection, indicating similar efficiencies of transfection and RNA replication from each construct (data not shown). As shown in Fig. 5A, we observed a slight delay in the kinetics of core protein release from cells transfected with the single-substitution genomes, S2428A, S2430A, and S2433A, up to 48 or 72 h posttransfection. However, core protein release from these cells reached comparable levels to that for the wild type at 96 h after transfection. In the cases of the double-substitution mutants (Fig. 5B), core protein release from cells transfected with the double-substitution genomes was markedly reduced, with 10- to 30-fold decreases compared to that for wild type observed. The kinetics of core protein release were similar to that for CL3B/SA.

Interaction of NS5A carrying single or double serine-to-alanine substitutions with the core protein was investigated by coimmunoprecipitation analysis using HA-tagged NS5A constructs. NS5A mutants carrying a single substitution were coimmunoprecipitated with the core protein (Fig. 5C), while none of the double-substitution NS5A mutants or the triple-substitution mutant, CL3B/SA, coimmunoprecipitated with the core protein (Fig. 5D). These results suggest that at least two serine residues in the C-terminal serine cluster of NS5A (aa 2428, 2430, and 2433) are necessary for the interaction between NS5A and the core protein as well as for regulation of HCV particle production and that there is positive correlation between their interaction and the amount of core protein released.

Glutamic acid partially substitutes for serine phosphorylation in the interaction of NS5A with the core protein and virus production. A consequence of phosphorylation is the addition of negative charge to a protein. In some cases, phosphoserine can be mimicked by glutamic or aspartic acid (14). To determine whether the introduction of negative charges into aa 2428, 2430, and 2433 instead of phosphoserines positively regulates the interaction of NS5A with the core protein and virus production, we replaced the serine residues with glutamic acid residues and constructed the CL3B/SE and S2428/2430E mutants (Fig. 6A). Cells transfected with the double-glutamic acid substitution, S2428/2430E, exhibited similar kinetics to the wild-type-transfected cells and released ~22-fold more core protein than S2428/2430A-transfected cells by 96 h posttransfection (Fig. 6B). In contrast,

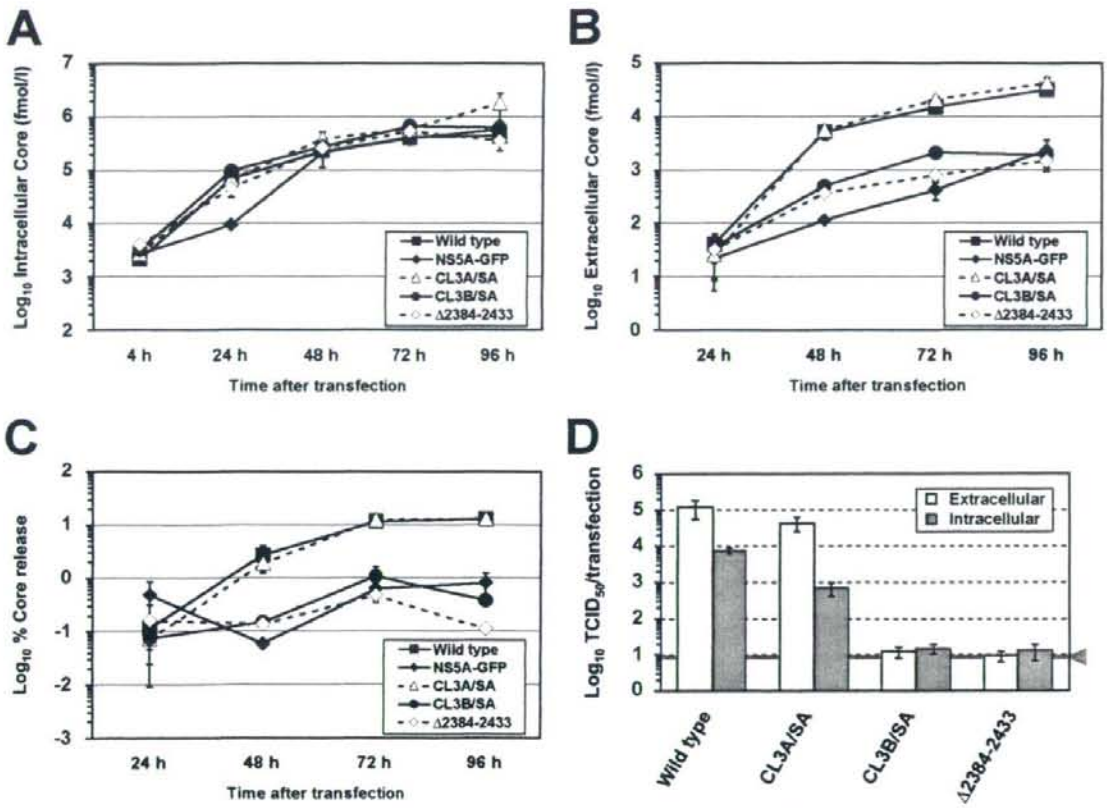

FIG. 3. Effect of mutations introduced into the NS5A C terminus on the production of infectious HCV particles. (A) Intracellular levels of core protein measured at various time points after transfection. A total of 3×10^6 Huh-7 cells were transfected with 10 μg of in vitro-transcribed HCV RNAs specified in the inset and resuspended in 10 ml of culture medium, after which 2-ml aliquots were seeded into each well of a six-well culture plate. The cells were harvested at different time points between 4 h and 96 h posttransfection, and then 500 μl of cell lysate per well was prepared. After centrifugation, supernatants were processed for a core protein-specific ELISA. (B) Release of core protein from cells transfected with the HCV genomes specified in the inset. Cell culture supernatants harvested from cells given in panel A were analyzed by a core protein ELISA. (C) Efficiency of core protein release from cells transfected with the HCV genomes specified in the inset. The percent core protein release (vertical axis) indicates the percentage of released core protein in relation to total core protein (the sum of intra- and extracellular core protein) calculated for each time point. (D) Infectivity of virus particles contained in supernatants and cells after transfection with mutants specified below the graph. Culture supernatants and cells were harvested 72 h posttransfection, and extracellular (white bars) and intracellular infectivity (gray bars) levels were determined by $TCID_{50}$ assay. The gray line and arrowhead represent the detection limit of the limiting dilution assay. Mean values and standard deviations for at least triplicates are shown in all panels.

the transfectant with the triple glutamic acid substitution, CL3B/SE, showed similar trends to that of CL3B/SA. In the coimmunoprecipitation experiments with FLAG-tagged core protein and HA-tagged NS5A constructs (Fig. 6C), S2428/2430E, but not S2428/2430A, restored the ability of NS5A to interact with the core protein up to a similar level to that of wild type. As expected, neither CL3B/SE nor CL3B/SA coimmunoprecipitated with the core protein. Taken together, these results indicate that negative charges at aa 2428 and 2430 preserve the ability of NS5A to interact with the core protein and positively regulate virus production. However, the data of the CL3B/SE mutant indicate that it is likely that negative charges alone are not sufficient to enhance either the interaction of NS5A with the core protein or virus production.

Subcellular localization of NS5A and core protein in Huh-7 cells expressing HCV genomes. The coimmunoprecipitation experiments described above indicate that the wild-type NS5A but not the CL3B/SA mutant interacts with the core protein. To evaluate the NS5A-core protein interaction in intact cells, we examined the subcellular localization of NS5A with the core protein by immunofluorescence analysis. NS5A colocalized with the core protein in cells transfected with the JFH-1 wild type (Fig. 7A), whereas their colocalization was rarely observed in cells transfected with the CL3B/SA RNA (Fig. 7B).

To further analyze the subcellular compartments for the localization of NS5A and core protein in cytoplasmic membrane structures, including the endoplasmic reticulum (ER) and LDs, we performed subcellular fractionation studies as

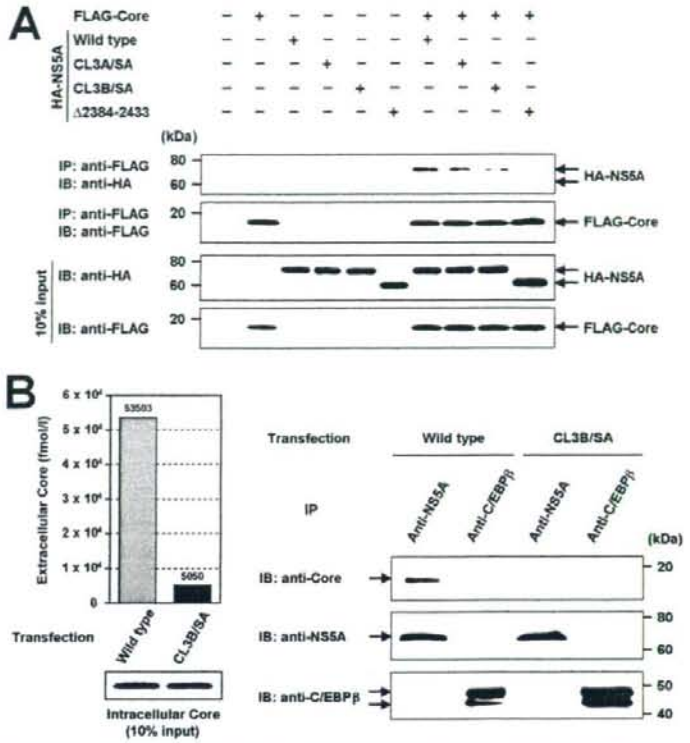

FIG. 4. aa 2428, 2430, and 2433 are essential for the interaction between NS5A and the core protein. (A) Effect of mutations at the NS5A C terminus on the interaction of NS5A with the core protein. N-terminally FLAG-tagged core protein and N-terminally HA-tagged NS5A carrying defined mutations were coexpressed in Huh-7 cells and immunoprecipitated with anti-FLAG antibody. The resulting precipitates were examined by immunoblotting using anti-HA or FLAG antibody. One-tenth of the cell lysates used in IP is shown as the 10% input. (B) Interaction between NS5A and the core protein in HCV-replicating cells. Huh-7 cells were lysed 72 h after transfection of the in vitro transcript of the HCV genome (wild type or CL3B/SA) and were immunoprecipitated with anti-NS5A antibody or anti-C/EBPβ antibody as a negative control. The resulting precipitates were examined by immunoblotting using anti-core protein, NS5A, or C/EBPβ antibody. One-tenth of cell lysates used in IP was immunoblotted with anti-core protein antibody (10% input). Cell culture supernatants harvested from transfected cells were analyzed by a core protein ELISA in parallel. IB, immunoblotting.

described in Materials and Methods. The iodixanol gradient was collected from the top to the bottom into 12 fractions (fractions 1 to 12). As shown in Fig. 7C, an ER marker, calnexin, was found in fractions 7 to 12 and was localized primarily in fractions 11 and 12. In contrast, ADRP, a cellular marker for LDs, was mainly observed in fractions 4 to 7. These two markers were equally distributed among cells analyzed (data not shown). The distribution of the wild-type NS5A was found in fractions 4 to 7, which was parallel to the fractionation profile of ADRP. The CL3B/SA-mutated NS5A was more broadly distributed and was also observed in heavier fractions than the wild-type NS5A, which was analogous to distribution of NS5A expressed in JFH1/4-1 cells bearing subgenomic replicons. The core protein in cells expressing the JFH-1 wild type, the CL3B/SA mutant, and in Huh/c-p7 cells that express JFH-1 structural proteins was distributed in a similar fashion, indicating that the distribution of core protein is not affected by NS5A mutation. The fractionation profile of the core protein, with a peak in fraction 4 or 5, was similar to that of the wild-type NS5A or ADRP but not to that of the CL3B/SA-mutated NS5A or calnexin, suggesting that core protein interacts with the wild-type NS5A in LD fractions, which is consistent with previous reports (33, 44, 45).

NS5A-core protein interaction is important for association of the core protein with the viral genomic RNA. To further address our hypothesis regarding involvement of NS5A in recruiting viral RNA to nucleocapsid formation, we analyzed the association of the core protein with HCV RNA in wild-type- or CL3B/SA-expressing cells by IP-RT-PCR (Fig. 8). Both cell lysates were immunoprecipitated with an anti-core protein antibody or a negative control, mouse IgG. Total RNA prepared from each immunoprecipitate was subjected to RT-PCR in order to detect HCV RNA. The amounts of immunoprecipitated core protein (Fig. 8, lower panel) as well as the expression of HCV RNA (Fig. 8, upper panels, Input) were comparable in both cells. In cells expressing the wild-type JFH-1 genome, the viral RNAs covering the 5′ terminal 2.2-kb as well as the 3′ terminal 2.2-kb regions were detected in immunopre-

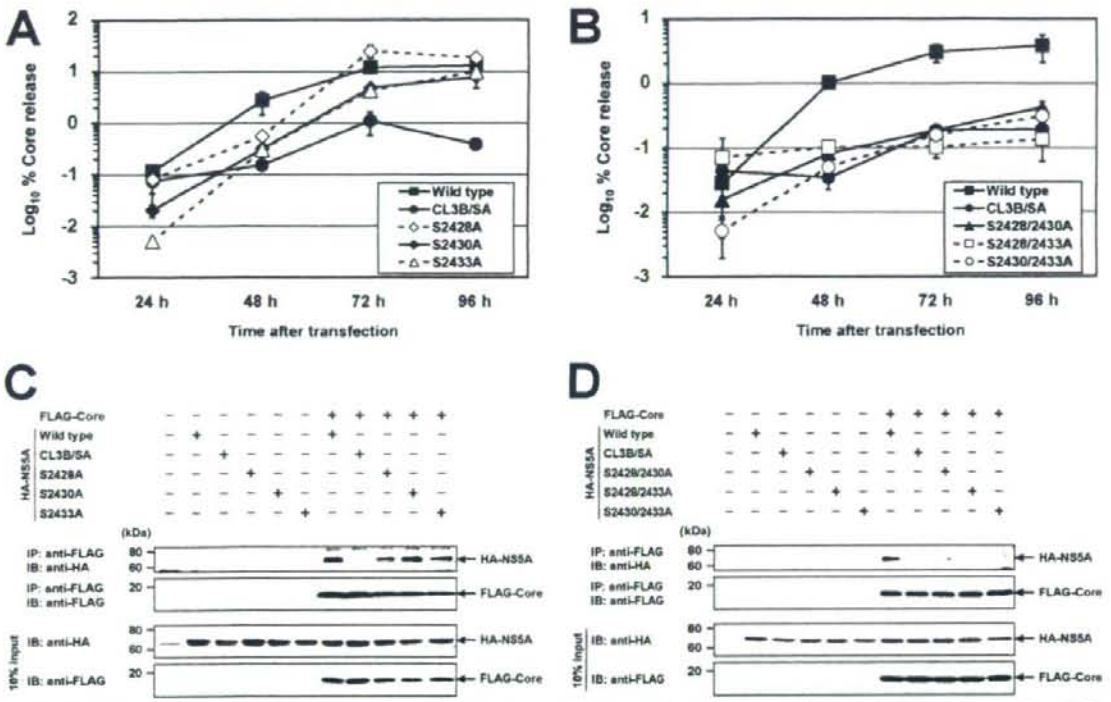

FIG. 5. Determination of critical amino acids responsible for virus production and the interaction of NS5A with the core protein. (A and B) Effect of single or double serine-to-alanine substitutions on virus production. After transfection of in vitro transcripts of the HCV genomes specified in the inset into Huh-7 cells, the cells and culture supernatants were harvested at the time points given, and the amounts of the core protein were determined by core protein-specific ELISA. Percent core protein release (vertical axis) indicates the percentage of released core protein in relation to total core protein (the sum of intra- and extracellular core protein) calculated for each time point. Mean values and standard deviations for at least triplicate experiments are shown. (C and D) Effect of single or double serine-to-alanine substitutions on the interaction between NS5A and the core protein. N-terminally FLAG-tagged core protein and N-terminally HA-tagged NS5A carrying defined mutations were coexpressed in Huh-7 cells and immunoprecipitated with anti-FLAG antibody. The resulting precipitates were examined by immunoblotting using anti-HA or FLAG antibody. One-tenth of the cell lysates used in IP is shown as the 10% input. IB, immunoblotting.

cipitates obtained with the anti-core protein antibody but not with the mouse IgG. In contrast, in cells expressing the CL3B/SA genome, HCV RNA was not detected in the immunoprecipitates with either antibody. These results demonstrate that HCV RNA associates with the core protein in cells where NS5A interacts with core protein (JFH-1 wild type) but not in cells where their interaction is impaired (CL3B/SA).

DISCUSSION

In the present study, we demonstrated the involvement of NS5A in the production of HCV particles via the interaction of NS5A with the core protein and identified its C-terminal serine cluster 3-B (aa 2428, 2430, and 2433), which is implicated in basal phosphorylation, as a key element for the interaction of NS5A with the core protein and for infectious virus production. Serine-to-alanine substitutions at the cluster, which have no impact on viral RNA replication, inhibit the interaction between NS5A and the core protein, thereby indicating that there is a connection between NS5A-core protein association and virus production. Finally, CL3B mutation leads to impairment of the association of the core protein with HCV RNA and, therefore, possibly RNA encapsidation.

Several reports have indicated that viral NS proteins are involved in the virion assembly of *Flaviviridae* viruses (25, 29, 30, 33). For instance, mutations in yellow fever virus NS2A block production of infectious virus, and this perturbation can be released by a suppressor mutation in NS3 (25), while the hydrophobic residues of Kunjin virus NS2A required for virus assembly have been mapped (26). Miyanari et al. have shown that HCV core protein recruits NS proteins to the LD-associated membranes and that the NS proteins around the LDs participate in the assembly of infectious viral particles (33). Furthermore, during preparation of the current article, two studies regarding participation of NS5A in the assembly of HCV particles were published. Appel et al. have demonstrated the essential role of domain III of NS5A in the formation of infectious particles, and deletions in this domain that disrupt colocalization of NS5A and the core protein abrogate virion production (2). Tellinghuisen et al. identified a serine residue in domain III as a key determinant for viral particle production

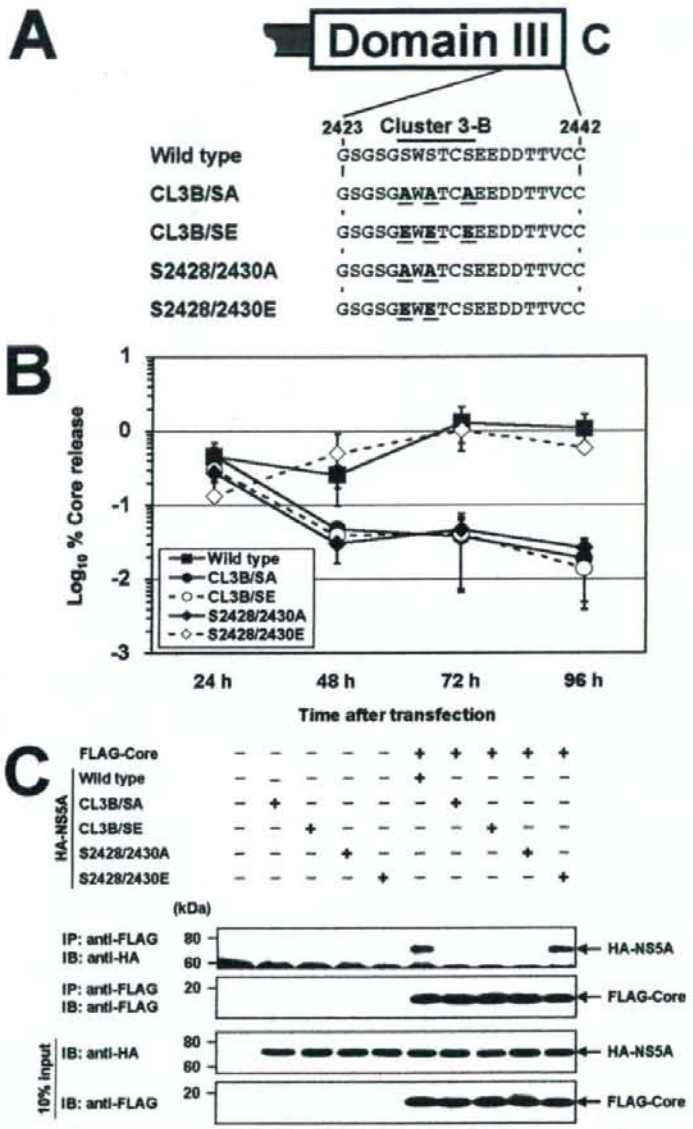

FIG. 6. Effect of glutamic acid substitutions for phosphoserines at aa 2428, 2430, and 2433 on virus production and the interaction of NS5A with the core protein. (A) Alanine or glutamic acid substitutions for serine residues at aa 2428, 2430, and 2433. The numbers indicate amino acid positions within the polyprotein of the JFH-1 isolate. The names shown on the left represent full-length HCV or N-terminally HA-tagged NS5A constructs used in this experiment. Amino acid substitutions are marked in bold and underlined. C represents the C terminus. (B) Effect of alanine or glutamic acid substitutions on virus production. After transfection of in vitro transcripts of the HCV genomes specified in the inset into Huh-7 cells, the cells and the culture supernatants were harvested at the time points given, and the amounts of core protein were determined by core protein-specific ELISA. Percent core protein release (vertical axis) indicates the percentage of released core protein in relation to total core protein (the sum of intra- and extracellular core protein) calculated for each time point. Mean values and standard deviations for at least triplicate experiments are shown. (C) Effect of alanine or glutamic acid substitutions on the interaction between NS5A and the core protein. N-terminally FLAG-tagged core protein and N-terminally HA-tagged NS5A carrying defined mutations were coexpressed in Huh-7 cells and immunoprecipitated with anti-FLAG antibody. The resulting precipitates were examined by immunoblotting (IB) using anti-HA or FLAG antibody. One-tenth of the cell lysates used in IP is as shown as the 10% input.

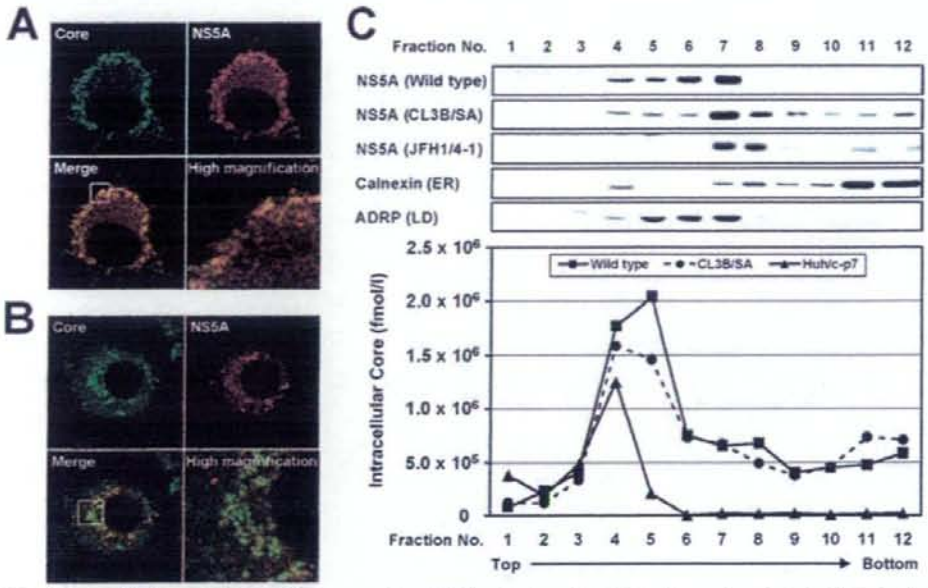

FIG. 7. Subcellular localization of NS5A and the core protein in HCV-replicating cells. Huh-7 cells were transfected with the in vitro transcript of the HCV genome, wild type (A) or CL3B/SA (B). Seventy-two hours after transfection, the cells were fixed with 4% paraformaldehyde, permeabilized with 0.3% Triton X-100, and double stained with antibodies against the core protein (green) and NS5A (red), followed by staining with an Alexa Fluor 488- or Alexa Fluor 555-conjugated antibody. High-magnification panels are enlarged images of white squares in the merge panels. (C) HCV (wild type or CL3B/SA)-replicating cells, JFH1/4-1 cells harboring a subgenomic replicon of JFH-1, or Huh/c-p7 cells stably expressing JFH-1 structural proteins were lysed by freeze-thawing, and the cell lysates were fractionated on 5 to 25% iodixanol gradients. The distributions of NS5A, calnexin (ER marker), and ADRP (LD marker) were determined by immunoblotting, and those of the core protein were examined by core protein-specific ELISA.

(50). However, the mechanism by which NS proteins participate in virus assembly or the role of the interaction between structural and NS proteins in virus life cycles has not been fully elucidated. Here, we have clearly demonstrated that HCV NS5A interacts with the core protein in coimmunoprecipitation experiments not only with coexpression of each epitope-tagged protein but also with cells expressing the viral genome; and by using immunofluorescence and subcellular fractionation analysis, we have confirmed that mutations in CL3B abolish colocalization of NS5A and the core protein, presumably around LDs. In addition, the intracellular infectivity assay and IP-RT-PCR strongly suggest that impairment of the NS5A-core protein interaction results in disruption of virus production at an early stage of virion assembly. On the basis of the present results and findings in accompanying articles, one may infer the following events: newly synthesized HCV RNAs bound to NS5A are released from the replication complex-containing membrane compartment and can be captured by the core protein via interaction with domain III of NS5A at the surface of LDs or LD-associated membranes. Consequently, the viral RNAs are encapsidated, and virion assembly proceeds in the local environment. Recruitment of newly synthesized viral RNAs to the core protein could be important for efficient nucleocapsid formation in cells, where concentrations of the viral genome and the structural proteins are typically low, and may contribute to the selection of the viral genome to be packaged. Interaction between NS5A and the core protein has been previously reported, and the NS5A region containing an interferon sensitivity determining region and the PKR-binding sequence (aa 2212 to 2330) has been mapped to that required for binding with core protein by yeast two-hybrid and in vitro pull-down assays (13). However, involvement of domain III in the NS5A-core protein interaction was not analyzed in detail, and a role for the NS5A-core protein interaction in the HCV life cycle was not examined in that study.

A growing body of evidence points to phosphorylation of NS5A as being important in controlling HCV RNA replication. Although the degree and the requirement for its hyperphosphorylation diverge between different HCV isolates, mutations that are associated with increased replicative fitness of HCV replicons frequently lead to a reduced level of NS5A hyperphosphorylation (1, 5, 36). Inhibitors of serine/threonine protein kinases that block NS5A hyperphosphorylation facilitate replication of a non-culture-adapted replicon (3, 36). One model that has been proposed suggests that NS5A hyperphosphorylation negatively regulates HCV RNA replication by disrupting the interaction between NS5A and the vesicle-associated membrane protein-associated protein subtype A, a cellular factor considered necessary for efficient RNA replication (5). However, the regulatory role of the basal phosphorylation of NS5A in the viral life cycle is poorly understood. It has been reported that the C-terminal region of NS5A (aa 2350 to 2419)

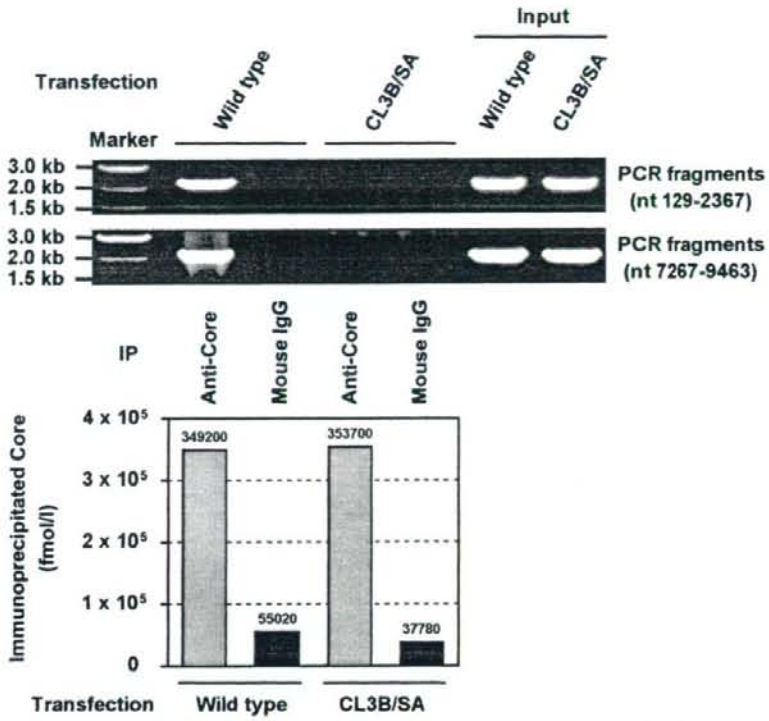

FIG. 8. IP-RT-PCR of HCV-replicating cells performed to examine the association between the core protein and the HCV genome RNA. Huh-7 cells were transfected with the in vitro transcript of the HCV genome (wild type or CL3B/SA) and lysed in 500 μl of hypotonic buffer at 72 h posttransfection. After IP with an anti-core protein antibody or mouse IgG, immunoprecipitates were eluted in 100 μl of elution buffer. RNAs in immunocomplexes were isolated by acid guanidinium thiocyanate-phenol-chloroform extraction. PCR was carried out as described in Materials and Methods with primer sets amplifying the fragments of nt 129 to 2367 and nt 7267 to 9463 of the JFH-1 genome. One-tenth (10 μl) of each eluted immunoprecipitate was used for assays of the core protein amounts to ensure IP efficiency (lower panel). RNA extracted from a small aliquot of each cell lysate used in IP-RT-PCR is shown as the input.

is involved in basal phosphorylation (23). There are highly conserved serine residues in this region, and alanine substitutions or in-frame deletion of the serine residues has been shown to impair basal phosphorylation but not to affect RNA replication in the genotype 1b isolate (1). Consistently, a metabolic ^{32}P labeling experiment in the present study demonstrated that NS5A mutants of the JFH-1 isolate in the region impair the basal phosphorylation. Nevertheless, Tellinghuisen et al. noted that the serine at aa 2433 of JFH-1 is involved in generating hyperphosphorylated NS5A, as shown by Western blotting (50). The basis for this difference is uncertain. To date, there is no clear evidence to determine which serine residues located in domain III are phosphoacceptor sites or whether these residues influence NS5A phosphorylation in an indirect fashion. Future study to map phosphoacceptor sites in the NS5A domain III by biochemical approaches is needed.

We found that two of the three serine residues at CL3B are responsible for regulating the interaction of NS5A with the core protein as well as for infectious virus production. To further evaluate the effect of constitutive serine phosphorylation at the cluster, we replaced the serine residues with glutamic acid, which mimics the presence of phosphoserines. The S2428/2430E mutant led to restoration of the interaction of NS5A with the core protein and virus production up to levels similar to the wild type. Somewhat unexpectedly, the triple glutamic acid substitution (CL3B/SE) exhibited only a slight restoration effect or none at all. It is considered that the degree of negative charge on the glutamic acid residue is not completely equivalent to that of phosphoserine. It is likely that the range of acidity at the local environment of the NS5A domain III that will allow interaction with the core protein is rather narrow. Induction of a conformational change in NS5A by the incorporation of phosphate may also be important for its interaction with the core protein. Tellinghuisen et al. reported that a single serine-to-alanine substitution at aa 2433 blocks the production of infectious virus and that casein kinase II likely phosphorylates the residue (50). Although this seems inconsistent with our results, these investigators also showed that deletions producing a lack of all three serine residues in the cluster inhibited virus production more severely than a single mutation. We observed that a single substitution of S2428A, S2430A, or S2433A resulted in a moderate decrease

in the virus released from the transfected cells; however, more evident perturbation was obtained from double or triple substitutions (Fig. 5A and B). Tellinghuisen et al. determined the HCV production at 48 h after RNA transfection and found a marked inhibition by the single substitution S2433A. In our study, as indicated in Fig. 5A, the reduction caused by the S2433A mutant was approximately 90% at 48 h after transfection; however, the virus production from the mutant reached a similar level to that of the wild type at 96 h posttransfection.

Several previous studies have found that apolipoproteins B (apoB) and E (apoE), microsomal triglyceride transfer protein, and HCV p7 protein are key factors for production of the infectious HCV particles (4, 11, 16, 22, 47). Assembly and maturation of the viral particles appear to depend on the formation of very-low-density lipoprotein, a large particle containing apoB, apoE, and large amounts of neutral lipids in hepatic cells. p7 protein is primarily involved in a late step of virus particle production, and the findings support the idea that p7 acts as viroporin, which has the capacity to compromise cell membrane integrity and thus favors the release of viral progeny. How the early step in virion production regulated by the NS5A-core protein interaction links with the later step(s) involved in the very-low-density lipoprotein assembly or p7 function remains an interesting question to be addressed.

In summary, we demonstrated that the C-terminal serine cluster of NS5A (aa 2428, 2430, and 2433), which is involved in generating the basal phosphorylated form, is a determinant of NS5A interaction with the core protein and the subcellular localization of NS5A. Mutation of this cluster blocks the NS5A-core protein interaction, resulting in perturbation of association between the core protein and HCV RNA. It is thus tempting to consider that NS5A plays a key role in transporting the viral genome RNA synthesized by the replication complex to the surface of LDs or LD-associated membranes, where the core protein localizes, leading to facilitation of nucleocapsid formation. Structural analysis of the NS5A domain III-core protein complex should provide greater insight into the mode of interaction between these viral proteins. Identification of residues at the interface that are involved in important interactions will be of significant value in designing novel structure-based inhibitors to block the early step of HCV particle formation.

ACKNOWLEDGMENTS

We are grateful to Francis V. Chisari (The Scripps Research Institute) for providing Huh-7 cells. We thank M. Matsuda, S. Yoshizaki, T. Shimoji, M. Kaga, and M. Sasaki for technical assistance and T. Mizoguchi for secretarial work.

This work was supported by Grants-in-Aid from the Ministry of Health, Labor and Welfare; by the Program for Promotion of Fundamental Studies in Health Sciences of the Organization for Drug ADR Relief, R&D Promotion and Product Review of Japan (grant ID:01-3); by the Japan Society for the Promotion of Science; and by Research on Health Sciences focusing on Drug Innovation from the Japan Health Sciences Foundation, Japan. T.M. is the recipient of a Research Resident Fellowship from the Foundation for Promotion of Cancer Research in Japan.

REFERENCES

1. **Appel, N., T. Pietschmann, and R. Bartenschlager.** 2005. Mutational analysis of hepatitis C virus nonstructural protein 5A: potential role of differential phosphorylation in RNA replication and identification of a genetically flexible domain. J. Virol. **79:**3187–3194.
2. **Appel, N., M. Zayas, S. Miller, J. Krijnse-Locker, T. Schaller, P. Friebe, S. Kallis, U. Engel, and R. Bartenschlager.** 2008. Essential role of domain III of nonstructural protein 5A for hepatitis C virus infectious particle assembly. PLoS Pathog. **4:**e1000035.
3. **Bürckstümmer, T., M. Kriegs, J. Lupberger, E. K. Pauli, S. Schmittel, and E. Hildt.** 2006. Raf-1 kinase associates with hepatitis C virus NS5A and regulates viral replication. FEBS Lett. **580:**575–580.
4. **Chang, K. S., J. Jiang, Z. Cai, and G. Luo.** 2007. Human apolipoprotein E is required for infectivity and production of hepatitis C virus in cell culture. J. Virol. **81:**13783–13793.
5. **Evans, M. J., C. M. Rice, and S. P. Goff.** 2004. Phosphorylation of hepatitis C virus nonstructural protein 5A modulates its protein interactions and viral RNA replication. Proc. Natl. Acad. Sci. USA **101:**13038–13043.
6. **Gale, M., Jr., C. M. Blakely, B. Kwieciszewski, S. L. Tan, M. Dossett, N. M. Tang, M. J. Korth, S. J. Polyak, D. R. Gretch, and M. G. Katze.** 1998. Control of PKR protein kinase by hepatitis C virus nonstructural 5A protein: molecular mechanisms of kinase regulation. Mol. Cell. Biol. **18:**5208–5218.
7. **Gale, M., Jr., and M. G. Katze.** 1998. Molecular mechanisms of interferon resistance mediated by viral-directed inhibition of PKR, the interferon-induced protein kinase. Pharmacol. Ther. **78:**29–46.
8. **Gale, M., Jr., B. Kwieciszewski, M. Dossett, H. Nakao, and M. G. Katze.** 1999. Antiapoptotic and oncogenic potentials of hepatitis C virus are linked to interferon resistance by viral repression of the PKR protein kinase. J. Virol. **73:**6506–6516.
9. **Gale, M. J., Jr., M. J. Korth, and M. G. Katze.** 1998. Repression of the PKR protein kinase by the hepatitis C virus NS5A protein: a potential mechanism of interferon resistance. Clin. Diagn. Virol. **10:**157–162.
10. **Gale, M. J., Jr., M. J. Korth, N. M. Tang, S. L. Tan, D. A. Hopkins, T. E. Dever, S. J. Polyak, D. R. Gretch, and M. G. Katze.** 1997. Evidence that hepatitis C virus resistance to interferon is mediated through repression of the PKR protein kinase by the nonstructural 5A protein. Virology **230:**217–227.
11. **Gastaminza, P., G. Cheng, S. Wieland, J. Zhong, W. Liao, and F. V. Chisari.** 2008. Cellular determinants of hepatitis C virus assembly, maturation, degradation, and secretion. J. Virol. **82:**2120–2129.
12. **Gastaminza, P., S. B. Kapadia, and F. V. Chisari.** 2006. Differential biophysical properties of infectious intracellular and secreted hepatitis C virus particles. J. Virol. **80:**11074–11081.
13. **Goh, P. Y., Y. J. Tan, S. P. Lim, S. G. Lim, Y. H. Tan, and W. J. Hong.** 2001. The hepatitis C virus core protein interacts with NS5A and activates its caspase-mediated proteolytic cleavage. Virology **290:**224–236.
14. **Hicke, L., B. Zanolari, and H. Riezman.** 1998. Cytoplasmic tail phosphorylation of the alpha-factor receptor is required for its ubiquitination and internalization. J. Cell Biol. **141:**349–358.
15. **Hoofnagle, J. H.** 2002. Course and outcome of hepatitis C. Hepatology **36:**S21–S29.
16. **Huang, H., F. Sun, D. M. Owen, W. Li, Y. Chen, M. Gale, Jr., and J. Ye.** 2007. Hepatitis C virus production by human hepatocytes dependent on assembly and secretion of very low-density lipoproteins. Proc. Natl. Acad. Sci. USA **104:**5848–5853.
17. **Huang, L., J. Hwang, S. D. Sharma, M. R. Hargittai, Y. Chen, J. J. Arnold, K. D. Raney, and C. E. Cameron.** 2005. Hepatitis C virus nonstructural protein 5A (NS5A) is an RNA-binding protein. J. Biol. Chem. **280:**36417–36428.
18. **Ishii, K., K. Murakami, S. S. Hmwe, B. Zhang, J. Li, M. Shirakura, K. Morikawa, R. Suzuki, T. Miyamura, T. Wakita, and T. Suzuki.** 2008. Trans-encapsidation of hepatitis C virus subgenomic replicon RNA with viral structure proteins. Biochem. Biophys. Res. Commun. **371:**446–450.
19. **Ishii, K., Y. Ueda, K. Matsuo, Y. Matsuura, T. Kitamura, K. Kato, Y. Izumi, K. Someya, T. Ohsu, M. Honda, and T. Miyamura.** 2002. Structural analysis of vaccinia virus DIs strain: application as a new replication-deficient viral vector. Virology **302:**433–444.
20. **Jesch, S. A., A. J. Mehta, M. Velliste, R. F. Murphy, and A. D. Linstedt.** 2001. Mitotic Golgi is in a dynamic equilibrium between clustered and free vesicles independent of the ER. Traffic **2:**873–884.
21. **Johnson, R. F., S. E. McCarthy, P. J. Godlewski, and R. N. Harty.** 2006. Ebola virus VP35-VP40 interaction is sufficient for packaging 3E–5E minigenome RNA into virus-like particles. J. Virol. **80:**5135–5144.
22. **Jones, C. T., C. L. Murray, D. K. Eastman, J. Tassello, and C. M. Rice.** 2007. Hepatitis C virus p7 and NS2 proteins are essential for production of infectious virus. J. Virol. **81:**8374–8383.
23. **Kaneko, T., Y. Tanji, S. Satoh, M. Hijikata, S. Asabe, K. Kimura, and K. Shimotohno.** 1994. Production of two phosphoproteins from the NS5A region of the hepatitis C viral genome. Biochem. Biophys. Res. Commun. **205:**320–326.
24. **Kato, T., T. Date, M. Miyamoto, M. Sugiyama, Y. Tanaka, E. Orito, T. Ohno, K. Sugihara, I. Hasegawa, K. Fujiwara, K. Ito, A. Ozasa, M. Mizokami, and T. Wakita.** 2005. Detection of anti-hepatitis C virus effects of interferon and ribavirin by a sensitive replicon system. J. Clin. Microbiol. **43:**5679–5684.
25. **Kümmerer, B. M., and C. M. Rice.** 2002. Mutations in the yellow fever virus nonstructural protein NS2A selectively block production of infectious particles. J. Virol. **76:**4773–4784.

26. **Leung, J. Y., G. P. Pijlman, N. Kondratieva, J. Hyde, J. M. Mackenzie, and A. A. Khromykh.** 2008. Role of nonstructural protein NS2A in flavivirus assembly. J. Virol. **82:**4731–4741.
27. **Liang, T. J., B. Rehermann, L. B. Seeff, and J. H. Hoofnagle.** 2000. Pathogenesis, natural history, treatment, and prevention of hepatitis C. Ann. Intern. Med. **132:**296–305.
28. **Lindenbach, B. D., M. J. Evans, A. J. Syder, B. Wolk, T. L. Tellinghuisen, C. C. Liu, T. Maruyama, R. O. Hynes, D. R. Burton, J. A. McKeating, and C. M. Rice.** 2005. Complete replication of hepatitis C virus in cell culture. Science **309:**623–626.
29. **Liu, W. J., H. B. Chen, and A. A. Khromykh.** 2003. Molecular and functional analyses of Kunjin virus infectious cDNA clones demonstrate the essential roles for NS2A in virus assembly and for a nonconservative residue in NS3 in RNA replication. J. Virol. **77:**7804–7813.
30. **Liu, W. J., P. L. Sedlak, N. Kondratieva, and A. A. Khromykh.** 2002. Complementation analysis of the flavivirus Kunjin NS3 and NS5 proteins defines the minimal regions essential for formation of a replication complex and shows a requirement of NS3 in *cis* for virus assembly. J. Virol. **76:**10766–10775.
31. **Manns, M. P., H. Wedemeyer, and M. Cornberg.** 2006. Treating viral hepatitis C: efficacy, side effects, and complications. Gut **55:**1350–1359.
32. **Miyamoto, M., T. Kato, T. Date, M. Mizokami, and T. Wakita.** 2006. Comparison between subgenomic replicons of hepatitis C virus genotypes 2a (JFH-1) and 1b (Con1 NK5.1). Intervirology **49:**37–43.
33. **Miyanari, Y., K. Atsuzawa, N. Usuda, K. Watashi, T. Hishiki, M. Zayas, R. Bartenschlager, T. Wakita, M. Hijikata, and K. Shimotohno.** 2007. The lipid droplet is an important organelle for hepatitis C virus production. Nat. Cell Biol. **9:**1089–1097.
34. **Moradpour, D., M. J. Evans, R. Gosert, Z. Yuan, H. E. Blum, S. P. Goff, B. D. Lindenbach, and C. M. Rice.** 2004. Insertion of green fluorescent protein into nonstructural protein 5A allows direct visualization of functional hepatitis C virus replication complexes. J. Virol. **78:**7400–7409.

34a. **Murakami, K., T. Kimura, M. Osaki, K. Ishii, T. Miyamura, T. Suzuki, T. Wakita, and I. Shoji.** 2008. Virological characterization of the hepatitis C virus JFH-1 strain in lymphocytic cell lines. J. Gen. Virol. **89:**1587–1592.

35. **National Institutes of Health.** 2002. NIH consensus statement on management of hepatitis C. NIH Consens. State. Sci. Statements **19:**1–46.
36. **Neddermann, P., M. Quintavalle, C. Di Pietro, A. Clementi, M. Cerretani, S. Altamura, L. Bartholomew, and R. De Francesco.** 2004. Reduction of hepatitis C virus NS5A hyperphosphorylation by selective inhibition of cellular kinases activates viral RNA replication in cell culture. J. Virol. **78:**13306–13314.
37. **Niwa, H., K. Yamamura, and J. Miyazaki.** 1991. Efficient selection for high-expression transfectants with a novel eukaryotic vector. Gene **108:**193–199.
38. **Pawlotsky, J. M.** 1999. Hepatitis C virus (HCV) NS5A protein: role in HCV replication and resistance to interferon-alpha. J. Viral Hepat. **6**(Suppl. 1): 47–48.
39. **Pawlotsky, J. M., G. Germanidis, A. U. Neumann, M. Pellerin, P. O. Frainais, and D. Dhumeaux.** 1998. Interferon resistance of hepatitis C virus genotype 1b: relationship to nonstructural 5A gene quasispecies mutations. J. Virol. **72:**2795–2805.
40. **Poynard, T., M. F. Yuen, V. Ratziu, and C. L. Lai.** 2003. Viral hepatitis C. Lancet **362:**2095–2100.
41. **Schaller, T., N. Appel, G. Koutsoudakis, S. Kallis, V. Lohmann, T. Pietschmann, and R. Bartenschlager.** 2007. Analysis of hepatitis C virus superinfection exclusion by using novel fluorochrome gene-tagged viral genomes. J. Virol. **81:**4591–4603.
42. **Seeff, L. B., and J. H. Hoofnagle.** 2003. Appendix: The National Institutes of Health Consensus Development Conference: management of hepatitis C 2002. Clin. Liver Dis. **7:**261–287.
43. **Seeff, L. B., and J. H. Hoofnagle.** 2002. National Institutes of Health Consensus Development Conference: management of hepatitis C: 2002. Hepatology **36:**S1–S2.
44. **Shavinskaya, A., S. Boulant, F. Penin, J. McLauchlan, and R. Bartenschlager.** 2007. The lipid droplet binding domain of hepatitis C virus core protein is a major determinant for efficient virus assembly. J. Biol. Chem. **282:**37158–37169.
45. **Shi, S. T., S. J. Polyak, H. Tu, D. R. Taylor, D. R. Gretch, and M. M. Lai.** 2002. Hepatitis C virus NS5A colocalizes with the core protein on lipid droplets and interacts with apolipoproteins. Virology **292:**198–210.
46. **Shirakura, M., K. Murakami, T. Ichimura, R. Suzuki, T. Shimoji, K. Fukuda, K. Abe, S. Sato, M. Fukasawa, Y. Yamakawa, M. Nishijima, K. Moriishi, Y. Matsuura, T. Wakita, T. Suzuki, P. M. Howley, T. Miyamura, and I. Shoji.** 2007. E6AP ubiquitin ligase mediates ubiquitylation and degradation of hepatitis C virus core protein. J. Virol. **81:**1174–1185.
47. **Steinmann, E., F. Penin, S. Kallis, A. H. Patel, R. Bartenschlager, and T. Pietschmann.** 2007. Hepatitis C virus p7 protein is crucial for assembly and release of infectious virions. PLoS Pathog. **3:**e103.
48. **Tan, S. L., and M. G. Katze.** 2001. How hepatitis C virus counteracts the interferon response: the jury is still out on NS5A. Virology **284:**1–12.
49. **Tanji, Y., T. Kaneko, S. Satoh, and K. Shimotohno.** 1995. Phosphorylation of hepatitis C virus-encoded nonstructural protein NS5A. J. Virol. **69:**3980–3986.
50. **Tellinghuisen, T. L., K. L. Foss, and J. Treadaway.** 2008. Regulation of hepatitis C virion production via phosphorylation of the NS5A protein. PLoS Pathog. **4:**e1000032.
51. **Tellinghuisen, T. L., K. L. Foss, J. C. Treadaway, and C. M. Rice.** 2008. Identification of residues required for RNA replication in domains II and III of the hepatitis C virus NS5A protein. J. Virol. **82:**1073–1083.
52. **Tellinghuisen, T. L., J. Marcotrigiano, A. E. Gorbalenya, and C. M. Rice.** 2004. The NS5A protein of hepatitis C virus is a zinc metalloprotein. J. Biol. Chem. **279:**48576–48587.
53. **Tellinghuisen, T. L., J. Marcotrigiano, and C. M. Rice.** 2005. Structure of the zinc-binding domain of an essential component of the hepatitis C virus replicase. Nature **435:**374–379.
54. **van den Hoff, M. J., A. F. Moorman, and W. H. Lamers.** 1992. Electroporation in "intracellular" buffer increases cell survival. Nucleic Acids Res. **20:**2902.
55. **van Regenmortel, M. H. V., C. M. Fauquet, D. H. L. Bishop, E. B. Carstens, M. K. Estes, S. M. Lemon, J. Maniloff, M. A. Mayo, D. J. McGeoch, C. R. Pringle, and R. B. Wickner (ed.).** 2000. Virus taxonomy: classification and nomenclature of viruses. Seventh report of the International Committee on Taxonomy of Viruses. Academic Press, San Diego, CA.
56. **Wakita, T., T. Pietschmann, T. Kato, T. Date, M. Miyamoto, Z. Zhao, K. Murthy, A. Habermann, H. G. Krausslich, M. Mizokami, R. Bartenschlager, and T. J. Liang.** 2005. Production of infectious hepatitis C virus in tissue culture from a cloned viral genome. Nat. Med. **11:**791–796.
57. **Watashi, K., M. Hijikata, A. Tagawa, T. Doi, H. Marusawa, and K. Shimotohno.** 2003. Modulation of retinoid signaling by a cytoplasmic viral protein via sequestration of Sp110b, a potent transcriptional corepressor of retinoic acid receptor, from the nucleus. Mol. Cell. Biol. **23:**7498–7509.
58. **Zhong, J., P. Gastaminza, G. Cheng, S. Kapadia, T. Kato, D. R. Burton, S. F. Wieland, S. L. Uprichard, T. Wakita, and F. V. Chisari.** 2005. Robust hepatitis C virus infection in vitro. Proc. Natl. Acad. Sci. USA **102:**9294–9299.

JOURNAL OF VIROLOGY, June 2008, p. 5715–5724 Vol. 82, No. 12
0022-538X/08/$08.00+0 doi:10.1128/JVI.02530-07

Critical Role of Virion-Associated Cholesterol and Sphingolipid in Hepatitis C Virus Infection▽

Hideki Aizaki,[1] Kenichi Morikawa,[1] Masayoshi Fukasawa,[2] Hiromichi Hara,[1] Yasushi Inoue,[1] Hideki Tani,[3] Kyoko Saito,[2] Masahiro Nishijima,[2] Kentaro Hanada,[2] Yoshiharu Matsuura,[3] Michael M. C. Lai,[4] Tatsuo Miyamura,[1] Takaji Wakita,[1] and Tetsuro Suzuki[1]*

Department of Virology II[1] and Department of Biochemistry and Cell Biology,[2] National Institute of Infectious Diseases, Tokyo 162-8640, and Department of Molecular Virology, Research Institute for Microbial Diseases, Osaka University, Osaka 565-0871,[3] Japan, and Department of Molecular Microbiology and Immunology, University of Southern California, Los Angeles, California 90033-1054[4]

Received 27 November 2007/Accepted 17 March 2008

In this study, we establish that cholesterol and sphingolipid associated with hepatitis C virus (HCV) particles are important for virion maturation and infectivity. In a recently developed culture system enabling study of the complete life cycle of HCV, mature virions were enriched with cholesterol as assessed by the molar ratio of cholesterol to phospholipid in virion and cell membranes. Depletion of cholesterol from the virus or hydrolysis of virion-associated sphingomyelin almost completely abolished HCV infectivity. Supplementation of cholesterol-depleted virus with exogenous cholesterol enhanced infectivity to a level equivalent to that of the untreated control. Cholesterol-depleted or sphingomyelin-hydrolyzed virus had markedly defective internalization, but no influence on cell attachment was observed. Significant portions of HCV structural proteins partitioned into cellular detergent-resistant, lipid-raft-like membranes. Combined with the observation that inhibitors of the sphingolipid biosynthetic pathway block virion production, but not RNA accumulation, in a JFH-1 isolate, our findings suggest that alteration of the lipid composition of HCV particles might be a useful approach in the design of anti-HCV therapy.

Hepatitis C virus (HCV) is recognized as a major cause of chronic liver disease, including chronic hepatitis, hepatic steatosis, cirrhosis, and hepatocellular carcinoma. It presently affects approximately 200 million people worldwide (26). HCV is an enveloped positive-strand RNA virus belonging to the *Hepacivirus* genus of the family *Flaviviridae*. Its genome of ~9.6 kb encodes a polyprotein precursor of ~3,000 residues, and the structural proteins (core, E1, and E2) reside in its N-terminal region.

Little is known about the assembly of HCV and its virion structure, because efficient production of authentic HCV particles has only recently been achieved. Nucleocapsid assembly generally involves oligomerization of the capsid protein and encapsidation of genomic RNA. This process is thought to occur upon interaction of the core protein with viral RNA, and this core-RNA interaction may induce a change from RNA replication to packaging. As with related viruses, the mature HCV virion likely consists of a nucleocapsid and an outer envelope composed of a lipid membrane and envelope proteins. Expression of the structural proteins in mammalian cells has been observed to generate virus-like particles with ultrastructural properties similar to those of HCV virions (5, 29). Packaging of these HCV-like particles into intracellular vesicles as a result of budding from the endoplasmic reticulum (ER) has also been observed (8, 34). However, HCV structural proteins are observed both in the ER and in the Golgi apparatus (45). Moreover, complex N-linked glycans have been detected on the surfaces of HCV particles isolated from patient sera, suggesting that the glycans transit through the Golgi apparatus (44). Interactions between the core and E1/E2 proteins are thought to determine viral morphology and are mediated through a cytoplasmic loop present in the polytopic form of E1 (35). Recently, we and others have identified a unique HCV genotype 2a isolate, JFH-1, that is able to replicate and produce high levels of infectious virus in culture (HCVcc) (54, 56), enabling us to investigate new aspects of the HCV life cycle.

In this study, we examine the importance of cholesterol and sphingolipid in association with the HCV membrane in virion maturation and virus infectivity. Mature HCV particles are rich in cholesterol. Cholesterol depletion or hydrolysis of sphingolipid from HCV particles results in a loss of infectivity. We further demonstrate a requirement for virion-associated cholesterol and sphingolipid for viral entry.

MATERIALS AND METHODS

Cell culture. The human hepatoma cell line Huh-7, which is permissive to HCV infection, was obtained from Francis V. Chisari (The Scripps Research Institute). Human embryonic kidney 293T cells were cultured in Dulbecco's modified Eagle medium (DMEM)–10% fetal bovine serum. Huh-7 cell lines, which carry subgenomic replicon RNA of either the JFH-1 (20) or the N (11, 17) strain, were cultured as previously described (21, 46).

Reagents. The primary antibodies used in this study were mouse monoclonal antibodies against vesicular stomatitis virus glycoprotein (VSV-G) (Sigma, St. Louis, MO), HCV E1 (54) and E2 (Biodesign International, Saco, ME), caveolin-2 (New England Biolabs, Beverly, MA), and CD81 (BD Pharmingen, Franklin Lakes, NJ), as well as rabbit polyclonal antibodies against calnexin (Stressgen, Ann Arbor, MI) and HCV core (48). ISP-1/myriocin, cholesterol, and

* Corresponding author. Mailing address: Department of Virology II, National Institute of Infectious Diseases, 1-23-1 Toyama, Shinjuku-ku, Tokyo 162-8640, Japan. Phone: 81 3 5285 1111. Fax: 81 3 5285 1161. E-mail: tesuzuki@nih.go.jp.

▽ Published ahead of print on 26 March 2008.

heparinase I were purchased from Sigma, and recombinant *Bacillus cereus* sphingomyelinase (SMase) was obtained from Higeta Shoyu (Tokyo, Japan). (*1R,3R*)-*N*-(3-Hydroxy-1-hydroxymethyl-3-phenylpropyl) dodecanamide (HPA-12), which was synthesized as described elsewhere (24), was a gift from Shu Kobayashi (University of Tokyo).

Plasmids. pCAE1 and pCAE2 contain HCV cDNAs spanning the E1 region (amino acids 192 to 383) with a FLAG tag at the N terminus and the E2 region (amino acids 384 to 809) with a Myc tag at the N terminus of strain NIHJ1 (1), respectively, under the control of the CAG promoter (38). pCAV340V and pCAV711V consist of the ectodomains of E1 and E2, respectively, with the N-terminal signal sequences, transmembrane domains, and cytoplasmic domains derived from VSV-G, as described elsewhere (50) (see Fig. 4D).

Virus production. Plasmid pJFH1, containing full-length cDNA of the JFH-1 isolate, was used to generate HCVcc as described elsewhere (23, 33, 34, 54). pJ6/JFH was obtained from JFH1 by replacement of the 5′ untranslated region to the p7 region (EcoRI-BclI) of J6. In vitro-transcribed RNA from linearized pJFH1 or pJ6/JFH1 was delivered to Huh-7 cells by electroporation. Culture supernatants were collected at 72 h posttransfection, clarified by low-speed centrifugation, passed through a 0.45-mm-pore-size filter, and concentrated using an Amicon Ultra-15 unit (Millipore, Bedford, MA) or by ultracentrifugation (23). Infectious titers, HCV RNA copies, and core protein concentrations of the viral stocks were $\sim 5 \times 10^3$ focus-forming units per ml, $\sim 1 \times 10^7$ copies/ml, and $\sim 1 \times 10^4$ fmol/liter, respectively. HCVcc was isolated by a combination of ultrafiltration, ion-exchange chromatography, heparin affinity chromatography, and sucrose density ultracentrifugation (33; K. Morikawa and T. Wakita, unpublished data). Pseudotyped VSV containing E1 and E2 proteins of the HCV genotype 1a isolate H77c (HCVpv) was generated as previously described (51). Briefly, 293T cells transiently expressing E1 and E2 proteins (strain H77) were infected with VSVdelG-GFP/G, in which the G envelope gene was replaced with green fluorescent protein (GFP) and pseudotyped with VSV-G.

Determination of cholesterol and phospholipid contents of HCVcc and infected cells. Cellular and viral lipids were extracted from isolated HCVcc and from uninfected and infected Huh-7 cells. Cholesterol content was determined using the cholesterol oxidase method as previously described (14). Total phospholipid content was determined using the method of Rouser et al. (42).

Cholesterol depletion and replacement. To remove cholesterol from the HCV envelope, stock samples of HCVcc were treated with *methyl*-β-cyclodextrin (B-CD) in DMEM (Sigma) supplemented with 10% fetal bovine serum (Sigma) and nonessential amino acids (Invitrogen, Carlsbad, CA) for 1 h at 37°C, followed by centrifugation at 100,000 × *g* for 3 h to form a pellet, which was resuspended in 0.5 ml of the medium. In order to replenish cholesterol, the medium of HCVcc treated with 5 mg/ml B-CD was replaced with DMEM containing various concentrations of exogenous cholesterol (Sigma) and incubated for 1 h, followed by centrifugation to form a pellet. In order to perform HCVcc infection assays, Huh-7 cells were infected with HCVcc, with or without the treatment described above, for 1 h at 37°C and then washed as described above. Viral core protein levels in the cells and in the supernatant were quantified 72 h later using an HCV core enzyme-linked immunosorbent assay (Ortho-Clinical Diagnostics, Tokyo, Japan).

SMase treatment. HCVcc was treated with SMase at various concentrations in DMEM for 1 h at 37°C and was then centrifuged at 100,000 × *g* for 3 h to form a pellet, which was resuspended in 0.5 ml of medium for the infection assays.

HCVcc binding and internalization assays. To monitor binding, cells grown in a 6-well plate were preincubated for 1 h at 4°C, after which B-CD- or SMase-treated HCVcc was bound to the cells for 1 h at 4°C. As a measure of virus internalization, following the virus binding procedure, the cells were warmed to 37°C and maintained for 2 h, after which they were treated with 0.25% trypsin for 10 min at 37°C. Huh7-25, a CD81-negative Huh-7 subclone (3), was used to ensure removal of surface-bound virus by trypsin treatment. For both the binding and internalization assays, the resulting cells, as described above, were washed with ice-cold phosphate-buffered saline, followed by lysis with TRIzol reagent (Invitrogen). Cell-associated virus was quantified by measuring the amount of HCV RNA in the cell lysate by the real-time reverse transcription-PCR method (2, 34). Cells were treated with heparinase as previously described (33).

HCV replication assay in HCVcc-infected or replicon cells. HCV subgenomic replicon cells or cells infected with HCVcc were treated with various concentrations of inhibitors for 72 h. Total RNA was isolated from replicon cells using TRIzol reagent (Invitrogen), followed by quantification of HCV RNA by real-time reverse transcription-PCR as previously described (2, 34). Levels of core protein in the culture supernatants of HCVcc-infected cells were tested as described above.

Detection of cholesterol content of HCVcc. For [^{3}H]cholesterol labeling of viruses, HCVcc-infected or uninfected cells were incubated with 50 mCi of [1α,2α-^{3}H]cholesterol in DMEM for 24 h. Culture supernatants of the cells were incubated in the presence or absence of B-CD at 5 mg/ml for 1 h at 37°C, followed by ultracentrifugation on a 60% sucrose cushion. The virus-containing fractions and corresponding fractions from an uninfected culture were lysed in the buffer containing 1% Triton X-100 (TX-100), and radioactivity was quantified by scintillation counting. Radioactivities (in counts per minute) of HCVcc samples were determined by subtracting the radioactivity of uninfected cells from that of HCVcc-infected cells.

TABLE 1. Cholesterol and phospholipid contents of HCVcc and cells

Cell type or virus	Content (nmol/mg of protein)[a]		Chol/PL ratio
	Chol	PL	
Cells			
Uninfected	105.9 ± 10.4	253.2 ± 10.6	0.42
JFH-1 infected	116.5 ± 10.0	292.0 ± 18.4	0.40
Virus			
JFH-1	43.6 ± 2.4	33.8 ± 1.8	1.29
J6/JFH-1[b]	28.7 ± 4.8	22.7 ± 2.9	1.26

[a] Data are averages of three independent measurements ± standard deviations. Chol, cholesterol; PL, phospholipids.

[b] J6/JFH1 virus was produced from the pJ6/N2X-JFH1 construct and has structural proteins from the J6CF strain.

Metabolic labeling analysis of sphingolipid content. After 2 h of incubation with [^{14}C]serine (0.5 mCi/ml) in Opti-MEM (Invitrogen), the cells were lysed with 0.1% sodium dodecyl sulfate, and total lipid was extracted with chloroform-methanol (1:2, vol/vol). The extracts were spotted onto silica gel 60 plates (Merck, Darmstadt, Germany) and chromatographed with methyl acetate–1-propanol–chloroform–methanol–0.25% KCl (25:25:25:10:9, vol/vol). Radioactive spots were quantitatively detected by BAS 2000 (Fuji Film, Japan).

Membrane flotation assay. The membrane flotation assay was performed as previously described (46).

RESULTS

Critical role of virion-associated cholesterol. A role of virion-associated cholesterol in infectivity has been demonstrated for several enveloped viruses (4). However, little is known about the role of lipids associated with the virions of flaviviruses, including HCV, and their contribution to the viral life cycle. To determine the lipid composition of mature HCV virions, we extracted total lipid from HCVcc (JFH-1 and chimeric J6/JFH-1) prepared from the culture supernatants of cells infected with HCV, as well as the total cellular membrane fractions of uninfected and infected Huh-7 cells. The cholesterol and phospholipid contents were quantified, because these are the two major lipid constituents of biological membranes. The cholesterol-to-phospholipid molar ratio, which is known as a parameter of membrane viscosity (47), was significantly higher in virus samples (1.29 and 1.26 for JFH-1 and J6/JFH-1, respectively) than in cell membrane samples (0.40 and 0.42 for JFH-1-infected and uninfected cells, respectively) (Table 1). The ratios in viral samples were similar to or greater than those in mammalian plasma membranes, where most cellular cholesterol is found. Minimal contamination of the viral samples with extracellular microvesicles likely occurred, since only a small amount of lipid was detected in a sample prepared from the culture medium of uninfected cells (data not shown). Thus, it is likely that HCV virions are enriched with cholesterol during assembly and maturation.

To investigate a potential role for the particular lipid composition of HCV particles, HCVcc was treated with

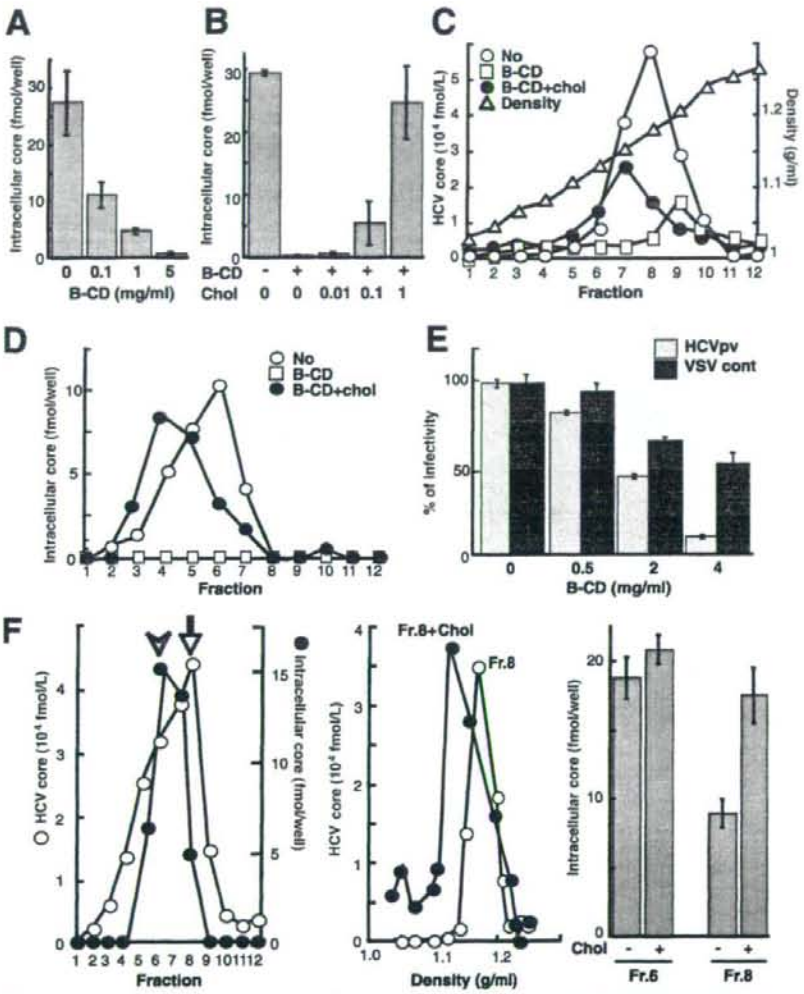

FIG. 1. Role of HCV-associated cholesterol in infection. (A) Effect of cholesterol depletion on HCV infectivity. HCVcc particles (~2 fmol of the core protein) were treated with B-CD at 0.1, 1, and 5 mg/ml for 1 h at 37°C. After removal of B-CD, Huh-7 cells were infected with the treated virus particles, after which the core protein content of infected cells at 72 h p.i. was determined as an indicator of infectivity, as previously established (24). (B) Effect of cholesterol replenishment on infectivity. After treatment with 5 mg/ml B-CD, virus was treated either with medium alone or with medium containing exogenous cholesterol for 1 h at 37°C. (C) Effect of cholesterol depletion and replenishment on density gradient profiles of the viral particles. The HCVcc treated with 5 mg/ml B-CD was replenished with exogenous cholesterol (1 mM) and then separated by 10-to-60% sucrose gradient ultracentrifugation. The core protein in each fraction was measured. The density of each fraction was determined by refractive index measurement. (D) Effects of cholesterol depletion and replenishment on viral infectivity. Each fraction (see panel C) was infected, and then the core proteins in the cells were measured at 72 h p.i. (E) Effect of cholesterol depletion on the infectivity of HCVpv (genotype 1a) (shaded bars) or the control, VSVdelG-GFP/G (solid bars). The viruses were preincubated with B-CD for 1 h at 37°C before infection. (F) (Left) The culture medium from HCVcc-producing cells was fractionated as described above. For each fraction, the amounts of core and intracellular core (infectivity) are plotted. Peaks of the core (arrow) and infectivity (arrowhead) are indicated. (Center) An aliquot of fraction 8 (peak of the core) was treated with 1 mM cholesterol for 1 h at 37°C. The resultant aliquot and an untreated aliquot of the fraction were subjected to sucrose gradient ultracentrifugation. The core in each fraction was plotted. (Right) The infectivities of fractions (Fr.) 6 and 8 (see the left panel) with or without cholesterol treatment were determined as shown above. Data are means from four independent experiments. Error bars, standard deviations.

increasing concentrations (0.1 to 5 mg/ml) of B-CD, which is known to extract cholesterol from membranes (40). The viral samples were then used to inoculate Huh-7 cells after removal of B-CD by ultracentrifugation. Infectivity was evaluated by quantifying the viral core protein in cells at 72 h postinfection (p.i.). Using an immunoassay that provides results indicative of HCV infectivity (25), we also confirmed a good correlation between the core level and

TABLE 2. Depletion of virion-associated cholesterol by B-CD

Treatment	Radioactivity (cpm) of HCVcc[a]		Avg (%[b])
	Expt 1	Expt 2	
None	5,327	5,573	5,450 (100)
B-CD (5 mg/ml)	3,643	1,646	2,644 (48.5)

[a] Determined by subtracting the radioactivity of uninfected cells from that of HCVcc-infected cells in two experiments.
[b] Percentage of the radioactivity of the untreated sample.

infectious titers (data not shown). As shown in Fig. 1A, core protein levels following B-CD treatment at 0.1, 1, or 5 mg/ml were reduced by 60, 83, or 98%, respectively, from the levels with the untreated virus. The cholesterol level of HCVcc treated with 5 mg/ml B-CD was found to be ~50% of that of untreated virions (Table 2).

To demonstrate that the reduced infection efficiency of B-CD-treated virus was caused by the reduced cholesterol content of the viral envelope, we attempted to reverse the inhibitory effect by adding exogenous cholesterol. Following treatment of HCVcc with 5 mg/ml B-CD, the drug was washed out, and increasing concentrations of cholesterol were added in an attempt to reconstitute the normal virion cholesterol content. The addition of 1 mM cholesterol completely reversed the virus infectivity (Fig. 1B). After cholesterol was replenished, the viral RNA was restored to a level similar to that in the untreated control.

To investigate the effect of cholesterol on the density of infectious HCV virions, B-CD-pretreated or untreated viral samples, as well as cholesterol-replenished treated viral samples, were subjected to sucrose density gradient centrifugation (Fig. 1C). The density of HCVcc core protein at its peak concentration in untreated virus samples was ~1.17 g/ml. When virion-associated cholesterol was removed by B-CD, the density of HCVcc core protein at its peak concentration was shifted to 1.20 g/ml. Addition of exogenous cholesterol to this cholesterol-depleted sample restored a lower-density fraction (1.15 g/ml). Figure 1D illustrates the infectivity of each gradient fraction. Untreated virus had maximum infectivity at ~1.13 g/ml (fraction 6), while, as expected, fractions from B-CD-treated viral samples exhibited minimal to no infectivity. Replenishment of depleted virus with cholesterol returned infectivity to untreated-control levels, and cholesterol-replenished virus had a buoyant density of ~1.07 g/ml (fraction 4), suggesting that HCV-associated cholesterol is crucial for viral infectivity and that the effect of a cholesterol-depleting drug is reversible. We further observed that B-CD treatment of a pseudotyped VSV containing the E1 and E2 proteins of the HCV genotype 1a isolate H77c (HCVpv) resulted in a progressive loss of infectivity, while B-CD had significantly less impact on the infectivity of the control virus VSVdelG-GFP/G (Fig. 1E).

The results described above raise the possibility that the infectivity of HCV virions with relatively low levels of incorporated cholesterol might be enhanced by supplementation with exogenous cholesterol. Density gradient fractions of culture supernatants collected from HCV-infected cells were analyzed with regard to the presence of core protein and infectivity (Fig. 1F, left). As indicated above, maximum infectivity was obtained with fraction 6 (1.13 g/ml). In contrast, a major fraction of core protein banded at a higher density (1.17 g/ml) in fraction 8. We hypothesized that fraction 8 contains lipids at lower levels than those in fraction 6. However, quantification of lipids, including cholesterol, in the fractions obtained failed, presumably due to a low sensitivity of detection. Thus, to extend our findings on the involvement of cholesterol, we added exogenous cholesterol to fraction 8, followed by ultrafiltration to remove unincorporated cholesterol. A subsequent density gradient profile demonstrated a shift in the core protein peak to 1.13 g/ml (Fig. 1F, center). A concomitant increase in the infectivity of the fraction, approaching that of untreated fraction 6, was observed (Fig. 1F, right). In contrast, supplementation of fraction 6 with exogenous cholesterol did not alter its infectivity (Fig. 1F, right) or change its density gradient (data not shown). These results suggest that exogenous cholesterol supplementation can reverse deficits in the infectivity of HCV virions due to low cholesterol content.

Sphingolipid dependence of HCV infectivity. In addition to cholesterol, sphingolipid is a major component of eukaryotic lipid membranes. We therefore investigated the functional significance of sphingomyelin (SM), the most abundant sphingolipid, with regard to HCV infectivity. HCVcc was treated for 1 h with increasing concentrations (0.1 to 10 U/ml) of bacterial SMase, which is known to hydrolyze membrane-bound SM to ceramide. Following ultracentrifugation to remove the SMase, Huh-7 cells were inoculated with the HCVcc. The amount of HCV core protein within the cells was quantified at 72 h p.i. Figure 2A shows 50 and 90% reductions in HCV infectivity after incubation of the virion with 0.1 and 1 U/ml SMase, respectively. We further observed that SMase treatment of HCVpv resulted in a progressive loss of infectivity, while SMase had no effect on the infectivity of the control virus (Fig. 2B). This demonstrates that sphingolipid, like cholesterol, plays an essential role in HCV infectivity.

Requirement for virion-associated cholesterol and sphingolipid during HCV cell entry. These findings support the idea that virion-associated cholesterol and sphingolipid may influence viral entry into host cells by altering the interaction between viral particles and a host cell factor(s). Viral entry is a multistep process including binding of the virion to the cell surface and internalization into the cytoplasm by endocytosis. To examine whether virion-associated cholesterol and SM might play a role in cell binding or postbinding events during viral entry, we used a binding assay in which Huh-7 cells preincubated for 1 h at 4°C were infected with B-CD- or SMase-treated HCVcc. Total RNA was extracted after a 1-h addition of the virions at 4°C, followed by quantification of HCV RNA. As shown in Fig. 3A, treatment of the virions with either B-CD or SMase had little influence on their ability to bind to cells.

It has been shown that CD81 plays an important role in HCV internalization but is not correlated with viral attachment (7, 33). An anti-CD81 antibody was used as a negative control for reduced viral attachment. It is likely that heparan sulfate proteoglycan on the target cell surface is needed for the initial attachment of HCV (33). Thus, heparinase I was used as a positive control for reduced HCV attachment to the cells. To examine the roles of cholesterol and sphingolipid on the HCVcc membrane in viral internalization, a virus-cell mixture

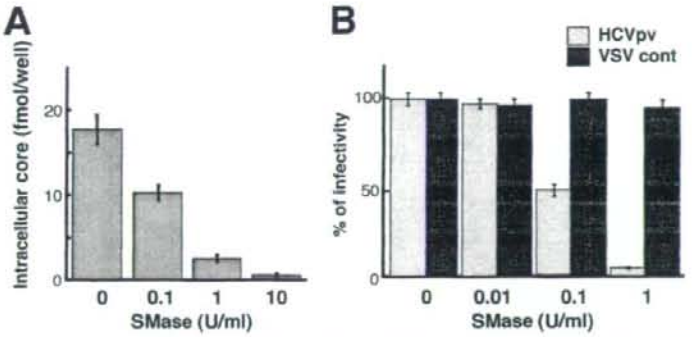

FIG. 2. Effect of SM hydrolysis on viral infectivity. (A) Effect on the infectivity of HCVcc. HCVcc was treated with 0.1, 1, or 10 U/ml SMase for 1 h at 37°C, after which SMase was removed by ultracentifugation. Huh-7 cells were infected with the treated virus, and the core protein content of infected cells was determined at 72 h p.i. (B) Effect on the infectivity of HCVpv (genotype 1a) (shaded bars) or the control, VSVdelG-GFP/G (VSV cont) (solid bars). The viruses were preincubated with SMase for 1 h at 37°C before infection. Data are means from four independent experiments. Error bars, standard deviations.

prepared at 4°C as described above was incubated for 2 h at 37°C, followed by trypsinization to remove virions that were surface bound but not internalized (Fig. 3B). We verified that 94% of surface-bound-viruses were removed by trypsinization using CD81-negative Huh-7 subclones. A marked reduction in viral RNA levels within cells was detected after pretreatment of the virus with either B-CD or SMase. These results strongly suggest that virion-associated cholesterol and sphingolipid function as key determinants of internalization but not of cell attachment.

Association of HCV structural proteins with lipid rafts. Cholesterol and sphingolipid are major components of lipid rafts, which can be isolated as detergent-resistant membranes (DRMs) by treatment with cold TX-100, followed by equilibrium flotation centrifugation. Matto et al. (30) reported that HCV core protein is associated with DRMs in cells carrying the full-length HCV replicon. To investigate whether HCV structural proteins are associated with DRMs in HCVcc-producing cells, lysates from cells infected with HCVcc were subjected to membrane flotation analysis. In the absence of detergent treatment, the majority of the core (Fig. 4A) and E1 (Fig. 4B) proteins were detected in the membrane fractions. After treatment with cold TX-100, significant amounts of both viral proteins were recovered from the DRM fraction. However, after treatment with TX-100 at 37°C, the majority of the E1 and core proteins had shifted to the detergent-soluble fractions. We also found that HCV genotype 1b E1 and E2 can be associated with the lipid raft in 293T cells transfected with an E1 or E2 expression plasmid (Fig. 4C) and that the cytoplasmic tails of envelope

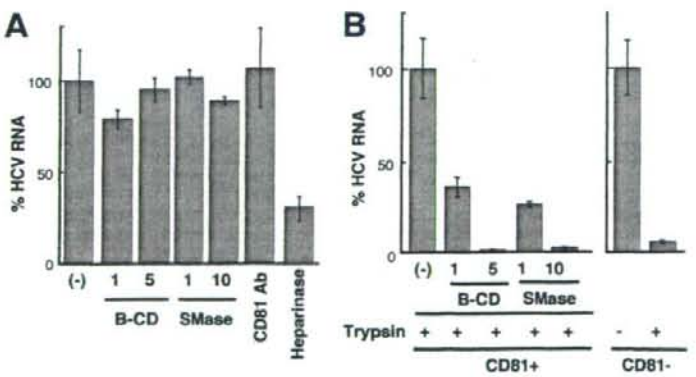

FIG. 3. Effects of B-CD or SMase on virus attachment and internalization. (A) Virus attachment to Huh-7 cells was determined at 4°C after treatment of HCVcc with B-CD (1 or 5 mg/ml) or SMase (1 or 10 U/ml). An antibody (Ab) against CD81 was used, in order to ensure that the antibody did not inhibit HCVcc binding (7, 33). Heparinase was used to reduce HCV attachment to the cell. Viral RNA copies were normalized to total cellular RNA, and the normalized RNA copies in the mock-treated sample (−) were arbitrarily set at 100%. (B) Virus internalization was measured in Huh7-25, a CD81-negative subclone (CD81$^-$) (3), and Huh7-25-CD81, which stably expresses CD81 (CD81$^+$), after treatment of the virions with B-CD or SMase. After internalization for 2 h at 37°C, cells were exposed to trypsin (trypsin +) or phosphate-buffered saline (trypsin −). Huh7-25 was used to ensure that surface-bound virus would be removed by trypsin treatment. The amounts of HCV RNA in Huh7-25 and Huh7-25-CD81 cells infected with untreated HCVcc were assigned the arbitrary value of 100%, respectively. Results are representative of four independent experiments.

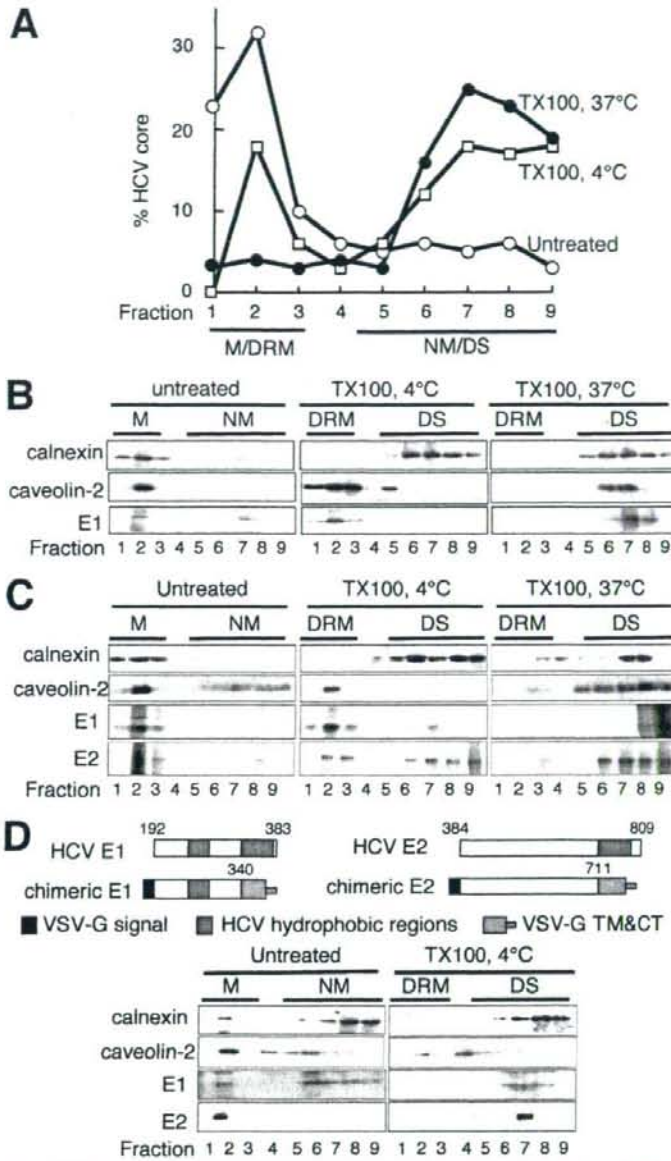

FIG. 4. Compartmentation of HCV structural proteins within DRM fractions. Lysates of HCVcc-infected cells were either treated with 1% TX-100, either on ice or at 37°C, or left untreated, followed by sucrose gradient centrifugation. (A and B) For each fraction, the amount of core protein was determined by an enzyme-linked immunosorbent assay (A), and E1, calnexin, and caveolin-2 were analyzed by Western blotting (B). The amount of core protein in each lysate (TX-100, 37°C; TX-100, 4°C; Untreated) was assigned the arbitrary value of 100%. M, membrane; NM, nonmembrane; DS, detergent soluble. (C) Lysates of 293T cells expressing HCV E1 or E2 protein were either treated with 1% TX-100, either on ice or at 37°C, or left untreated, followed by discontinuous sucrose gradient centrifugation. Each fraction was concentrated in a Centricon YM-30 filter unit and subjected to 12.5% sodium dodecyl sulfate-polyacrylamide gel electrophoresis, followed by immunoblotting with antibodies against calnexin, caveolin-2, Myc (E1), or FLAG (E2). (D) (Top) Structures of HCV envelope genes used. Amino acid positions of HCV are indicated. Signal sequence, transmembrane (TM), and cytoplasmic tail (CT) domains of VSV G protein are shown. (Bottom) Cell lysates expressing chimeric HCV E1 or E2 protein were treated with 1% TX-100 on ice or left untreated, followed by discontinuous sucrose gradient centrifugation. It has been reported that VSV-G is not associated with lipid (39). Calnexin, caveolin-2, and chimeric glycoproteins (chimeric E1 and chimeric E2) were analyzed by immunoblotting. Fractions are numbered from 1 to 9 in order from top to bottom (light to heavy).

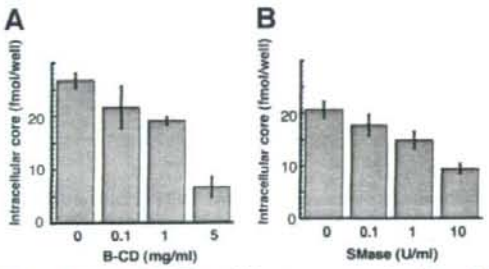

FIG. 5. Effects of B-CD or SMase treatment of cells on HCV infectivity. Huh-7 cells were either left untreated or treated with B-CD at 0.1, 1, or 5 mg/ml (A) or with SMase at 0.1, 1, or 10 U/ml (B) prior to HCVcc infection. Intracellular core levels were quantitated 72 h p.i. Data are means from four independent experiments. Error bars, standard deviations.

proteins are important for their interaction (Fig. 4D). These data suggest that subpopulations of HCV structural proteins are associated with lipid rafts in cells generating the HCV particles.

Moderate inhibition of HCV infection by B-CD or SMase treatment of host cells. It has recently been reported that cholesterol depletion or SM hydrolysis from the host cell membrane decreases HCV infection, in part by decreasing the level of CD81 on the cell surface (19, 53). The involvement of the lipid environment of the host cell plasma membrane in HCV infection was investigated in our HCVcc infection system. Prior to infection, Huh-7 cells were treated with B-CD or SMase and then washed with the medium five times. Cholesterol depletion from Huh-7 cells by B-CD at 1 or 5 mg/ml inhibited HCV core levels by 20 and 75%, respectively, compared to levels in untreated cells (Fig. 5A). We also found that hydrolysis of SM by SMase at 1 or 10 U/ml on the cells, respectively, led to moderate reduction of the viral infection, by 20 or 55% of the infection level of the untreated control (Fig. 5B). There was no influence on cell viability under the conditions of these treatments (data not shown). These findings, compared with the results in Fig. 1A and 2A, suggest that the raft-like environment on the plasma membrane likely serves as a portal for HCV entry, but HCV virion-associated cholesterol and sphingolipid more readily play more critical roles in viral infection.

Inhibitors of the sphingolipid biosynthetic pathway suppress the production of HCVcc, but not RNA replication, for a JFH-1-derived replicon. In the course of studying the involvement of lipid metabolism in the HCV life cycle, we observed that inhibitors of the sphingolipid biosynthetic pathway, including ISP-1 and HPA-12, which specifically inhibit serine palmitoyltransferase (31) and ceramide trafficking from the ER to the Golgi apparatus (55), influenced subgenomic replicons derived from the HCV-N isolate (genotype 1b), but not those derived from JFH-1. A dose-dependent decrease in HCV RNA copy numbers among HCV-N replicon cells was observed upon exposure to ISP-1 or HPA-12, as previously reported (43, 52). In contrast, these compounds had little or no effect on viral RNA accumulation in JFH-1 replicon cells (Fig. 6A). Furthermore, these compounds did not affect luciferase activity in the lysates of Huh-7 cells transfected with an in vitro-transcribed JFH-1 replicon RNA containing a luciferase reporter gene (22) (data not shown). Figure 6B shows the effects of ISP-1 and HPA-12 on de novo sphingolipid biosynthesis by replicon cells. No differences in the inhibitory effects of each compound were observed in replicon cells derived from HCV-N versus JFH-1. When de novo synthesis of sphingolipids was examined by metabolic labeling with [^{14}C]serine, ISP-1 almost completely inhibited the production of both ceramide and SM, while HPA-12 greatly inhibited the synthesis of SM but not ceramide. Levels of phosphatidylethanolamine and phosphatidylserine, into which serine is incorporated by a pathway distinct from that of sphingolipid biosynthesis, were not influenced by these drugs. These results suggest that suppression of HCV RNA replication by inhibitors of sphingolipid biosynthesis might be dependent on the viral genotype or isolate.

This observation prompted us to investigate whether inhibitors of the sphingolipid biosynthetic pathway might have the ability to prevent HCV virion production. Interestingly, when Huh-7 cells producing JFH-1 HCVcc were treated with ISP-1 or HPA-12 under conditions similar to those the replicon cells, viral core levels in the culture supernatants were greatly reduced in a dose-dependent manner. For example, exposure to 10 μM ISP-1 or 1 μM HPA-12 reduced viral core protein levels more than 85% from those for control cells (Fig. 6C). The 50% inhibitory concentrations of both drugs were less than 0.1 μM, 50-fold less than those obtained for the RNA replication of the HCV-N-replicon. Together, these results suggest that the sphingolipid biosynthetic pathway plays an important role in the production of HCV particles, but not in genome replication, in JFH-1-based HCVcc.

DISCUSSION

In this study, we demonstrated the role of HCV virion-associated cholesterol and sphingolipid in viral infectivity. Although dependence on virion-associated cholesterol for virus entry has been shown for a number of viruses (4, 6, 28, 49), this is the first study to demonstrate the importance of envelope cholesterol in a virus belonging to the family *Flaviviridae*. Furthermore, to our knowledge, the functional role of virion membrane-associated SM has not been examined in viruses. Our previous studies using Chinese hamster ovary cell mutants deficient in SM synthesis have demonstrated that reduction of cellular SM levels enhances cellular cholesterol efflux in the presence of B-CD (9, 12). Thus, it may be possible that SM plays a role in the retention of cholesterol on HCV particles due to interaction between cholesterol and SM. The finding that B-CD or SMase treatment of HCVcc markedly inhibited virus internalization but not cell attachment (Fig. 3) suggests that HCV membrane-associated cholesterol and sphingolipid are crucial for the interaction of viral glycoproteins with the virus-receptor/coreceptor required for cell entry. Cholesterol depletion or sphingolipid hydrolysis might induce a conformational change in the viral envelope, resulting in instability of the virion structure. Since the cholesterol/phospholipid ratios of membranes affect bilayer fluidity, the maturation of viral envelopes with high cholesterol/phospholipid ratios via association with rafts may be important for the stability of HCV

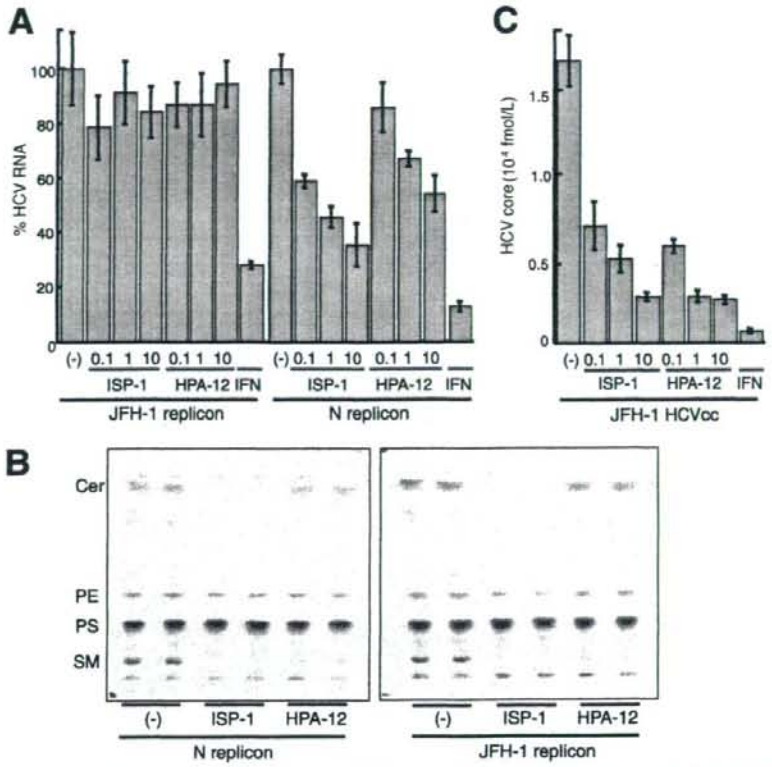

FIG. 6. Anti-HCV effects of inhibitors of the sphingolipid biosynthetic pathway. Subgenomic replicon cells derived from HCV isolate N or JFH-1, as well as HCVcc-producing cells, were treated with ISP-1 (0.1, 1, or 10 μM), HPA-12 (0.1, 1, or 10 μM) or alpha interferon (IFN) (100 U/ml) for 72 h. HCV RNA titers in the replicon cells (A) and the HCV core protein content of the culture medium of infected cells (C) were determined. Data are means from four independent experiments. Error bars, standard deviations. (B) De novo synthesis of sphingolipid in the absence or presence of ISP-1 (10 μM) and HPA-12 (10 μM) was monitored in duplicate by metabolic labeling with [^{14}C]serine for 2 h at 37°C. Cer, ceramide; PE, phosphatidylethanolamine; PS, phosphatidylserine.

particles. Replenishing the viral membrane with cholesterol following treatment with 5 mg/ml B-CD successfully restored viral infectivity to the same level as that of untreated virus (Fig. 1), suggesting that reversible B-CD-induced changes in HCV structure might critically influence viral infectivity. However, we were unable to restore viral infectivity by replenishing cholesterol after pretreatment of the virion with concentrations of B-CD exceeding 10 mg/ml (data not shown). Under these conditions, it is likely that large holes in the viral membrane destroy the virus, a result that cannot be reversed by supplying exogenous cholesterol.

How are cholesterol and sphingolipid involved in the HCV virion during the process of virus maturation? Like most positive-stranded RNA viruses, HCV is thought to assemble at the ER membrane. However, Miyanari et al. (32) reported that lipid droplets are important for HCVcc formation. These authors have shown that the characteristics of lipid-droplet-associated membranes in Huh-7 cells differ from those of ER membranes. In the case of flaviviruses, for which the mechanism of viral assembly and budding remains unclear (15), a few studies have demonstrated budding at the plasma membrane (13, 36, 37, 41), and it has been proposed that the site of budding may be virus and cell type dependent (27). We demonstrate here that subpopulations of HCV structural proteins partition into cellular detergent-resistant, lipid-raft-like membrane fractions in HCVcc-producing cells (Fig. 4) and that inhibitors of the sphingolipid biosynthetic pathway block HCV virion production (Fig. 6). Furthermore, a large proportion of HCV E2 protein incorporated into HCVcc is endoglycosidase H resistant (data not shown). Thus, membrane compartments containing cholesterol- and sphingolipid-rich microdomains may be involved in HCV virion maturation. Another explanation for the recruitment of these lipids to the HCV membrane may be an association between the virus and very-low-density lipoprotein (VLDL) or low-density lipoprotein. Recently, Huang et al. (16) demonstrated a close link between HCV production and VLDL assembly, suggesting that an HCV-VLDL complex is generated and secreted from cells.

Recent reports have demonstrated that CD81-mediated HCV infection is partly dependent on cell membrane choles-